Inorganic Chemistry

Article

pubs.acs.org/IC

Synthesis and Characterization of $V^{IV}O$ Complexes of Picolinate and Pyrazine Derivatives. Behavior in the Solid State and Aqueous Solution and Biotransformation in the Presence of Blood Plasma Proteins

Tanja Koleša-Dobravc,[†] Elzbieta Lodyga-Chruscinska,[‡] Marzena Symonowicz,[‡] Daniele Sanna,[§] Anton Meden,[†] Franc Perdih,*[,†] and Eugenio Garribba*[,⊥]

[†]Faculty of Chemistry and Chemical Technology, University of Ljubljana, Aškerčeva cesta 5, SI-1000 Ljubljana, Slovenia, and CO EN−FIST, Dunajska cesta 156, SI-1000 Ljubljana, Slovenia

[‡]Institute of General Food Chemistry, Technical University of Lodz, ul. Stefanowskiego 4/10, Lodz, Poland

[§]Istituto CNR di Chimica Biomolecolare, Trav. La Crucca 3, I-07040 Sassari, Italy

[⊥]Dipartimento di Chimica e Farmacia and Centro Interdisciplinare per lo Sviluppo della Ricerca Biotecnologica e per lo Studio della Biodiversità della Sardegna, Università di Sassari, Via Vienna 2, I-07100 Sassari, Italy

Supporting Information

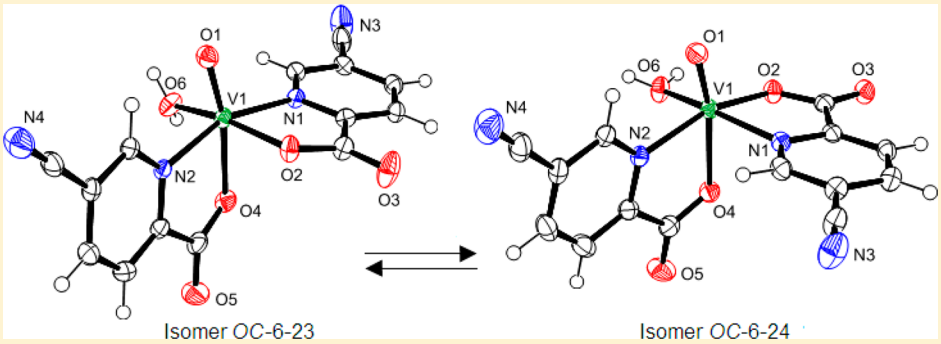

ABSTRACT: Oxidovanadium(IV) complexes with 5-cyanopyridine-2-carboxylic acid (HpicCN), 3,5-difluoropyridine-2-carboxylic acid (HpicFF), 3-hydroxypyridine-2-carboxylic acid (H_2hypic), and pyrazine-2-carboxylic acid (Hprz) have been synthesized and characterized in the solid state and aqueous solution through elemental analysis, IR and EPR spectroscopy, potentiometric titrations, and DFT simulations. The crystal structures of the complexes (*OC*-6-23)-[VO(picCN)$_2$(H_2O)]·2H_2O (**1**·2H_2O), (*OC*-6-24)-[VO(picCN)$_2$(H_2O)]·4H_2O (**2**·4H_2O), (*OC*-6-24)-Na[VO(Hhypic)$_3$]·H_2O (**4**), and two enantiomers of (*OC*-6-24)-[VO(prz)$_2$(H_2O)] (Λ-**5** and Δ-**5**) have been determined also by X-ray crystallography. **1** presents the first crystallographic evidence for the formation of a *OC*-6-23 isomer for bis(picolinato) $V^{IV}O$ complexes, whereas **2**, **4**, and **5** possess the more common *OC*-6-24 arrangement. The strength order of the ligands is H_2hypic ≫ HpicCN > Hprz > HpicFF, and this results in a different behavior at pH 7.40. In organic and aqueous solution the three isomers *OC*-6-23, *OC*-6-24, and *OC*-6-42 are formed, and this is confirmed by DFT simulations. In all the systems with apo-transferrin (VO)$_2$(apo-hTf) is the main species in solution, with the hydrolytic $V^{IV}O$ species becoming more important with lowering the strength of the ligand. In the systems with albumin, (VO)$_x$HSA (x = 5, 6) coexists with VOL$_2$(HSA) and VOL(HSA)(H_2O) when L = picCN, prz, with [VO(Hhypic)(hypic)]$^-$, [VO(hypic)$_2$]$^{2-}$, and [(VO)$_4$(μ-hypic)$_4$(H_2O)$_4$] when H_2hypic is studied, and with the hydrolytic $V^{IV}O$ species when HpicFF is examined. Finally, the consequence of the hydrolysis on the binding of $V^{IV}O^{2+}$ to the blood proteins, the possible uptake of V species by the cells, and the possible relationship with the insulin-enhancing activity are discussed.

INTRODUCTION

Vanadium compounds show a wide variety of pharmacological properties, including antiparasitic, spermicidal, antiviral, anti-HIV, antituberculosis, and antitumor activity.[1] One of the most important applications of V derivatives in medicine is the potential use in the therapy of patients suffering from type 2 diabetes mellitus,[2] which affects worldwide more than 100 million people according to the estimates of World Health Organization (but it is expected that this number will pass 350 million in 2030[3]). Type 2 diabetes, which depends on the body's inability to respond to insulin produced in the pancreas,

Received: April 1, 2014
Published: July 11, 2014

   dx.doi.org/10.1021/ic500766t | *Inorg. Chem.* 2014, 53, 7960−7976

represents approximately 90% of the cases.[4] A class of very promising complexes consists of neutral $V^{IV}O$ species with bidentate anionic ligands L^- (with L named also organic carrier) with composition VOL_2; for example, [VO-(maltolato)$_2$], or BMOV, is the benchmark compound for the new molecules with antidiabetic action.[5] $V^{IV}O$ complexes are more effective in lowering the glucose concentration in blood serum than the parent salt $VOSO_4$ and are well tolerated in all the animal models of diabetes. One derivative of BMOV, [VO(ethylmaltolato)$_2$], or BEOV, has completed phases I and IIa of clinical trials,[6] even if these have provisionally been abandoned due to renal problems arising with several patients and to the financial problems of Akesis Pharmaceuticals, Inc.[1a,7] Therefore, the recent efforts have been oriented toward the synthesis of new compounds with high activity and low toxicity: the incorporation of an antioxidant group in the structure of the organic ligand[8] and coadministration of vanadate(V) in an herbal decoction[9] gave promising results. It has been noticed that the balance of lipo- and hydrophilicity as well as the stability at low pH of the stomach play an important role in the uptake and pharmacological efficiency of V compounds.[3,10] Recently, a $V^{IV}O$ complex formed by allixin, a constituent of garlic *Allium sativum* L., has been demonstrated to be particularly active when administered to mice affected by diabetes induced with streptozotocin (STZ) by both intraperitoneal injections and oral administration.[11]

$V^{IV}O$ species with $VO(N_2O_2)$ coordination appeared to be very effective in the treatment of insulin-dependent diabetes mellitus.[12] In 1995 [VO(pic)$_2$(H$_2$O)] (pic = picolinate) was found to be a strong inhibitor of fatty acid mobilization and active in the treatment of STZ-induced diabetic rats.[13] Subsequently, it was shown that the complex formed by the methyl derivative of picolinate, [VO(6-methylpicolinato)$_2$], exhibits better *in vitro* insulin-enhancing and *in vivo* hypoglycemic effect in STZ-rats than the parent [VO-(pic)$_2$(H$_2$O)].[14] Subsequently, several $V^{IV}O$ complexes formed by picolinate derivatives were tested, such as [VO(2-quinolinecarboxylato)$_2$],[12a] [VO(3-methylpicolinato)$_2$],[15] [VO(5-iodopicolinato)$_2$],[16] *trans*-[VO(6-ethylpicolinato)$_2$(H$_2$O)],[17] *cis*-[VO(3-hydroxypicolinato)$_2$(H$_2$O)],[18] *cis*-[VO(5-carbomethoxypicolinato)$_2$(H$_2$O)],[19] and the bis-chelated *cis*-octahedral species formed by 2,5-dipicolinic acid and its monoesters.[20] The functionalization of 2,5-dipicolinate with an amino acid lowers significantly the value of IC_{50} (which defines the concentration of V compound required to inhibit 50% of the FFA release from the isolated rat adipocytes treated with epinephrine).[21] The Crans/Willsky team showed that also V^{III}, $V^{IV}O$, and $V^{V}O_2$ complexes of 1,6-dipicolinate are very promising in the lowering of blood glucose.[22]

The biotransformation of the antidiabetic complexes in the blood is an important aspect of the drug metabolism, but the mechanism with which vanadium is transported to the target organs and the *in vivo* form are not fully known and have been recently reviewed.[23] In the plasma the interaction with the proteins plays a key role, and the binding of potential antidiabetic $V^{IV}O$ drugs to transferrin (hTf) (in the form of both apo- and holo-transferrin), albumin (HSA), and immunoglobulin G (IgG) was demonstrated in the literature by several groups.[24−27] There is a general consensus that, when the arrangement of a V compound in aqueous solution at pH 7.40 is *cis*-octahedral and specific sites are not available for $V^{IV}O^{2+}$, species with the stoichiometry *cis*-VOL_2(Proteins) are formed through the coordination of an accessible His-N[25,26b,27c−i] or Asp-COO$^-$,[28] which replaces the water molecule in the fourth equatorial position. The knowledge of the complexation scheme, the thermodynamic stability of the species formed, and the biotransformation in the blood serum of the potentially active solid V compounds is fundamental to understand which is the active species in the organism.[29]

In this work we synthesized and characterized five potential antidiabetic compounds formed by three picolinic and one pyrazine derivative (Scheme 1) with the $V^{IV}O^{2+}$ ion. The characterization was carried out through the combined application of X-ray diffraction analysis, spectroscopic (EPR, IR), and computational (DFT) methods. The stability of the $V^{IV}O$ species in aqueous solution was evaluated by potentiometric titrations. Finally, the interaction of bis-chelated $V^{IV}O$ complexes with apo-transferrin and albumin was studied by EPR spectroscopy.

Scheme 1. Ligands Studied in This Work

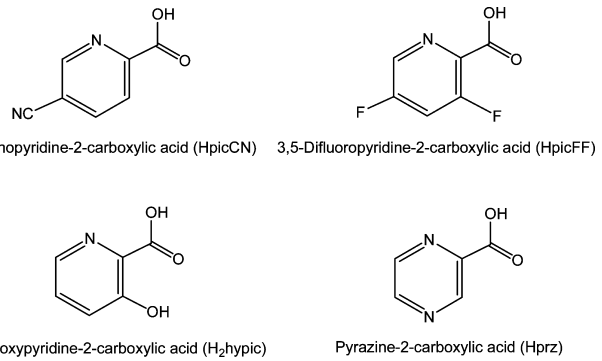

EXPERIMENTAL AND COMPUTATIONAL SECTION

Materials. $VOSO_4·5H_2O$ (Acros Organics), $VOSO_4·3H_2O$ (Aldrich), 5-cyanopyridine-2-carboxylic acid (5-cyanopicolinic acid, or HpicCN, Aldrich), 3,5-difluoropyridine-2-carboxylic acid (3,5-difluoropicolinic acid, or HpicFF, Aldrich), 3-hydroxypyridine-2-carboxylic acid (3-hydroxypicolinic acid, or H_2hypic, Alfa Aesar), pyrazine-2-carboxylic acid (Hprz, Fluka), calcium acetate hydrate (Fluka), sodium acetate trihydrate (Carlo Erba), methanol (Lab-Scan), ethanol (Carlo Erba), and acetone (J. T. Baker) were reagent grade and used as purchased without any further purification. Other chemicals, 4-(2-hydroxyethyl)piperazine-1-ethanesulfonic acid (HEPES), 1-methyimidazole (1-MeIm), and $NaHCO_3$, were Aldrich products of the highest grade available and used as received. Human serum apo-transferrin (98%, T4283) and human serum albumin (97−99%, A9511) were purchased from Sigma. The concentration of the protein solutions was estimated from their UV absorption (ε_{280}(apo-hTf) = 92 300 M^{-1} cm^{-1};[30] ε_{279}(HSA) = 35 300 M^{-1} cm^{-1} [31]).

Synthesis. *Synthesis of [VO(picCN)$_2$(H$_2$O)]·2H$_2$O (1·2H$_2$O).* A suspension of 5-cyanopyridine-2-carboxylic acid (1.00 mmol, 148 mg) and calcium acetate hydrate (0.50 mmol, 79 mg) in methanol (4 mL) was added dropwise to a solution of $VOSO_4·5H_2O$ (0.50 mmol, 127 mg) in water (2 mL). The mixture was stirred at 70 °C for 1 h and was then allowed to cool to room temperature. The green precipitate formed was filtered off and suspended in a methanol/ethanol mixture (10 mL, 1:1), and the undissolved white part was filtered off and discarded. After addition of water (5 mL) to the remaining green solution and partial evaporation of solvents, a green powder precipitated. It was filtered off and dried. Yield: *m* = 119 mg (57.3%). Anal. Calcd for $C_{14}H_{12}N_4O_8V$ (415.21): C, 40.50; H, 2.91; N, 13.49. Found: C, 40.54; H, 2.84; N, 13.31. IR (ATR, cm^{-1}): 3386br, 3104w, 3057w, 3043w, 2920br, 2243w, 1684m, 1655s, 1601m, 1561w, 1475w, 1387w, 1333s, 1290m, 1248m, 1211w, 1151w, 1048m, 972s, 893w, 865w, 806m, 790m, 687s, 676s.

dx.doi.org/10.1021/ic500766t | Inorg. Chem. 2014, 53, 7960−7976

*Synthesis of [VO(picCN)$_2$(H$_2$O)]·4H$_2$O (**2**·4H$_2$O).* A small amount of crystals of **2**·4H$_2$O was isolated manually from a concomitant mixture of **1**·2H$_2$O and **2**·4H$_2$O obtained by a slow evaporation at room temperature of a solution prepared by dissolving **1**·2H$_2$O in hot water. Due to quick dehydration of **2**·4H$_2$O outside the solution, an amorphous solid was formed. Elemental analysis of the amorphous product indicates the loss of three equivalents of water molecules. Anal. Calcd for $C_{14}H_{10}N_4O_7V$ (397.20): C, 42.34; H, 2.54; N, 14.11. Found: C, 42.11; H, 2.37; N, 13.95. IR (ATR, cm^{-1}): 3564w, 3385w, 3061br, 2245m, 1691m, 1651s, 1606m, 1573w, 1479w, 1388m, 1361m, 1316s, 1290m, 1252m, 1211w, 1150w, 1047m, 973s, 870s, 803s, 684s.

*Synthesis of [VO(picFF)$_2$(H$_2$O)] (**3**).* A suspension of 3,5-difluoropyridine-2-carboxylic acid (1.00 mmol, 159 mg) and calcium acetate hydrate (0.50 mmol, 79 mg) in methanol (4 mL) was added dropwise to a solution of VOSO$_4$·5H$_2$O (0.50 mmol, 127 mg) in water (2 mL). The mixture was stirred at 70 °C for 1 h; thereafter ethanol (4 mL) was added and the mixture was allowed to cool to room temperature. A white precipitate was filtered off, and the remaining solution was concentrated to a small volume (~2 mL). After addition of acetone (5 mL), the precipitated green powder was filtered off and dried. Yield: *m* = 130 mg (64.8%). Anal. Calcd for $C_{12}H_6F_4N_2O_6V$ (387.15): C, 35.93; H, 1.51; N, 6.98. Found: C, 35.78; H, 1.62; N, 6.73. IR (ATR, cm^{-1}): 3378br, 3064w, 1676w, 1625m, 1600s, 1473w, 1431w, 1404m, 1329m, 1248s, 1131s, 970s, 890w, 846m, 679m, 624s.

*Synthesis of Na[VO(Hhypic)$_3$]·H$_2$O (**4**).* A suspension of 3-hydroxypyridine-2-carboxylic acid (1.08 mmol, 150 mg) and sodium acetate trihydrate (1.08 mmol, 147 mg) in methanol (5 mL) was added dropwise to a solution of VOSO$_4$·5H$_2$O (0.36 mmol, 91 mg) in water (1 mL). The mixture was stirred at 60 °C for 20 min and was then allowed to cool to room temperature. A white precipitate was filtered off, and the solution was concentrated to obtain a dark green crystalline product, which was filtered off and dried. Yield: *m* = 109 mg (58.0%). Anal. Calcd for $C_{18}H_{14}N_3NaO_{11}V$ (522.25): C, 41.40; H, 2.70; N, 8.05. Found: C, 41.60; H, 2.58; N, 7.89. IR (ATR, cm^{-1}): 3513w, 3391w, 2972br, 1647s, 1606w, 1571w, 1454s, 1402m, 1327m, 1307m, 1300m, 1250s, 1218s, 1127w, 1058w, 967s, 895m, 824m, 798m, 690s, 669m, 616w.

*Synthesis of [VO(prz)$_2$(H$_2$O)] (**5**).* A solution of pyrazine-2-carboxylic acid (2.00 mmol, 248 mg) and calcium acetate hydrate (1.00 mmol, 158 mg) in methanol (4 mL) was added dropwise to a solution of VOSO$_4$·5H$_2$O (1.00 mmol, 253 mg) in water (2 mL). The mixture was stirred at 70 °C for 1 h and was then allowed to cool to room temperature. A white precipitate was filtered off, and the solution was concentrated to obtain a green powder, which was filtered off and dried. Yield: *m* = 189 mg (57.1%). Anal. Calcd for $C_{10}H_8N_4O_6V$ (331.14): C, 36.27; H, 2.44; N, 16.92. Found: C, 36.32; H, 2.26; N, 16.92. IR (ATR, cm^{-1}): 2844br, 1670s, 1630m, 1594m, 1476w, 1422m, 1374m, 1321s, 1288w, 1163s, 1058m, 1053m, 981s, 864s, 790m, 737w, 723w, 661w.

Potentiometric Measurements. The stability constants of proton and $V^{IV}O^{2+}$ complexes in the systems containing HpicCN and HpicFF were determined by potentiometric titrations on 2.0 mL of sample. The ligand to metal molar ratio was in the range 1:1−15:1, and $V^{IV}O^{2+}$ concentration in the range 5.0 × 10^{-4}−1.0 × 10^{-3} M. Titrations were performed from pH 2.2 until precipitation or very extensive hydrolysis by adding carbonate-free NaOH of known concentration (ca. 0.1 M).[32] Measurements were carried out at 25.0 ± 0.1 °C and at a constant ionic strength of 0.2 M (KCl) with a MOLSPIN pH-meter equipped with a digitally operated syringe (Molspin DSI 0.250 mL) controlled by a computer. The values of pH were measured with a Russel CMAWL/S7 semimicro combined electrode, calibrated for hydrogen ion concentration by the method of Irving et al.[33] Purified argon was bubbled through the samples to ensure the absence of oxygen. The number of experimental points was 125 for each titration curve, and the reproducibility of the points included in the evaluation was within 0.005 pH unit in the whole pH range measured. The pK_W calculated from strong acid−strong base titrations was 13.75 ± 0.01.

The stability of the complexes, reported as the logarithm of the overall formation constant $\beta_{pqr} = [(VO)_pL_qH_r]/[VO]^p[L]^q[H]^r$, where VO stands for $V^{IV}O^{2+}$ ion, L is the deprotonated form of the ligands, and H is the proton, were calculated with the aid of the SUPERQUAD programs.[34] Standard deviations were calculated by assuming random errors. Hydroxido complexes of $V^{IV}O^{2+}$ were taken into account, and the following species were assumed: $[VO(OH)]^+$ (log β_{10-1} = −5.94), $[(VO)_2(OH)_2]^{2+}$ (log β_{20-2} = −6.95), with stability constants calculated from the data of Henry et al.[35] and corrected for the different ionic strengths by use of the Davies equation,[36] $[VO(OH)_3]^-$ (log β_{10-3} = −18.0), and $[(VO)_2(OH)_5]^-$ (log β_{20-5} = −22.0).[37] The standard deviations of the stability constants are given in parentheses in Table 3.

Spectroscopic and Analytical Measurements. Infrared (IR) spectra (4000−600 cm^{-1}) of the solid samples were recorded using a PerkinElmer Spectrum 100, equipped with a Specac Golden Gate Diamond ATR as a solid sample support. Elemental (C, H, N) analysis was obtained using a PerkinElmer 2400 Series II CHNS/O elemental analyzer. Anisotropic EPR spectra, recorded on frozen solutions (120 K) with an X-band (9.4 GHz) Bruker EMX spectrometer equipped with an HP 53150A microwave frequency counter, were obtained dissolving compounds **1**−**5** in DMF, MeOH, or VOSO$_4$·3H$_2$O and the ligand in water. As usual for the analysis of the EPR spectra, in all the figures reported in this study only the high-field region is presented, the part more sensitive to the identity and the amount of the several species in solution.

Preparation of the Solutions Containing Proteins for EPR Measurements. The solutions were prepared dissolving in ultrapure water (obtained through the purification system Millipore Milli-Q Academic) the solid $V^{IV}O$ compound (**1**−**5**) to obtain a concentration of the metal ion of 5.0 × 10^{-4} M in the systems with apo-hTf and 1.0 × 10^{-3} M in those with HSA. Argon was bubbled through the solutions to ensure the absence of oxygen and avoid the oxidation of the $V^{IV}O^{2+}$ ion. In the systems with apo-hTf, the pH was raised to ca. 4.0 and HEPES and NaHCO$_3$ were added to obtain final concentrations of 1.0 × 10^{-1} and 2.5 × 10^{-2} M. Subsequently, apo-hTf was added at pH 5.10 or 6.70 to obtain an apo-hTf/$V^{IV}O$ ratio of 2, and finally, the pH was brought to 7.40. In the systems with HSA, the pH was raised to ca. 5.0 and HEPES and HSA were added to obtain a concentration of 1.0 × 10^{-1} and 2.5 × 10^{-4} M. Finally, the pH was brought to 7.40. In both systems, the EPR spectra were immediately measured. The spectra were obtained without the addition of DMSO, and to increase the signal-to-noise ratio, signal averaging was used.[27a] Studies performed on the model systems prove that HEPES does not interact with the $V^{IV}O^{2+}$ ion at the conditions used for the experiments.

X-ray Diffraction Analysis. Crystals suitable for X-ray analysis were obtained from methanol/water solutions (2:1 for **1**·2H$_2$O and **5** and 5:1 for **4**) or from a water solution (**2**·4H$_2$O) at room temperature by slow evaporation of the solvents over a few days. Despite many attempts, no crystals of compound **3** suitable for X-ray analysis could be prepared. Single-crystal X-ray diffraction data were collected on Agilent Technologies SuperNova Dual diffractometer with an Atlas detector and Mo Kα radiation (λ = 0.71073 Å) at 150 K (**1** and **2**) and at 293 K (**4**) and Cu Kα radiation (λ = 1.54184 Å) at 293 K (Λ-**5** and Δ-**5**). The data were processed using CrysAlis Pro.[38] The structures were solved by direct methods using the program SHELXS-97[39] (**1**, Λ-**5**, Δ-**5**) or SIR97[40] (**2**, **4**) and refined on F^2 using full-matrix least-squares procedures (SHELXL-97).[39] All non-hydrogen atoms were refined anisotropically. Water molecules O9 and O10 in **2**·4H$_2$O are disordered over two positions with the fixed occupancy ratio 0.50:0.50, and ISOR instruction was used on O9B and O10B atoms of water molecules for proper refinement. The hydrogen atoms on aromatic rings and OH groups were treated as riding atoms in geometrically idealized positions. Hydrogen atoms attached to water oxygen atoms were readily located from difference Fourier maps and were refined fixing the bond lengths and isotropic temperature factors as U_{iso}(H) = 1.5U_{eq}(O). Hydrogen atoms on O9 and O10 in **2**·4H$_2$O were not found in the difference Fourier maps and were not included in the

dx.doi.org/10.1021/ic500766t | Inorg. Chem. 2014, 53, 7960−7976

refinement. Crystallographic data are listed in Table S1 of the Supporting Information.

DFT Calculations. All the DFT calculations described were performed with Gaussian 03 (revision C.02) software.[41] The structures of the isomers *OC*-6-23, *OC*-6-24, *OC*-6-42, and *OC*-6-44 of the species $[VOL_2(H_2O)]$ (L = picCN, picFF, prz) and of the ternary species formed by picCN, prz, and 1-MeIm (isomer *OC*-6-24 of VOL_2(MeIm), $VOL(H_2O)$(MeIm), and VOL(OH)(MeIm), L = picCN, prz) were optimized in the gas phase with the hybrid exchange-correlation functional B3P86 and the basis set 6-311G. This choice ensures a good degree of accuracy in the prediction of the structures of first-row transition metal complexes[42] and, in particular, of vanadium compounds.[43] For all the structures, minima were verified through frequency calculations.

The ^{51}V ***A*** tensor was calculated with the functional BHandHLYP (as incorporated in Gaussian) and the 6-311G(d,p) basis set with Gaussian 03 software according to the procedures previously published.[44] It must be taken into account that for a $V^{IV}O^{2+}$ species A_z is usually negative, but in the literature its absolute value is often reported. At first approximation, the ^{51}V hyperfine coupling tensor A has two contributions: the isotropic Fermi contact (A^{iso}) and the anisotropic or dipolar hyperfine interaction (A^D): $A = A^{iso}\mathbf{1} + A^D$, where **1** is the unit tensor. The values of the ^{51}V anisotropic hyperfine coupling constants along the *x*, *y* and *z* axes are $A_x = A^{iso} + A_x^D$, $A_y = A^{iso} + A_y^D$, and $A_z = A^{iso} + A_z^D$. The theory background was described in detail in refs 44c and 44e. The percent deviation from the experimental value, $|A_z|^{exptl}$, was calculated as follows: $100 \times [(|A_z|^{calcd} - |A_z|^{exptl})/|A_z|^{exptl}]$ (see Table 2).

The relative stability of the *cis*-octahedral isomers *OC*-6-23, *OC*-6-24, *OC*-6-42, and *OC*-6-44 of $[VOL_2(H_2O)]$ (L = picCN, picFF, prz) was calculated at the B3P86/6-311++G(d,p) and B3LYP/6-311++G(d,p) level of theory computing the solvent effect with the PCM[45] model, available in Gaussian 03 software. The performances of PCM were well established in the literature.[44d,h,i,46] The total value of the free energy in aqueous solution (G^{tot}_{aq}) for each species can be separated into the electronic plus nuclear repulsion energy (E^{ele}), the thermal contribution (G^{therm}), and the solvation free energy (ΔG^{solv}): $G^{tot}_{aq} = E^{ele} + G^{therm} + \Delta G^{solv}$. The free energy in the gas phase (G^{tot}_{gas}) can be found by neglecting the term ΔG^{solv}: $G^{tot}_{gas} = E^{ele} + G^{therm}$. The thermal contribution was estimated using the ideal gas model and the calculated harmonic vibrational frequencies to determine the correction due to zero-point energy and to the thermal population of the vibrational levels.[44d,h]

RESULTS AND DISCUSSION

1. Literature Data and Possible Geometry for Bis-chelated $V^{IV}O$ Complexes of Picolinate and Pyrazine Derivatives. Bis-chelated oxidovanadium(IV) complexes have three possible structural variations, depending on the presence or absence of a coordinated solvent molecule, such as water, and its position in the complex. Particularly, *cis*-octahedral, *trans*-octahedral, and square pyramidal structures are expected (Scheme 2).

The X-ray determination of the structures of $V^{IV}O$ complexes formed by HpicCN, H_2hypic, and Hprz (see below) indicate that, among the possible bis-chelated species shown in Scheme 2, the square pyramidal and *trans*-octahedral arrangements are less stable than the *cis*-octahedral ones, and preliminary DFT results confirm this assumption. For (N, O) ligands, such as those studied in this work, four isomers are possible for the *cis*-octahedral geometry (Scheme 3).

Scheme 2. Possible Bis-chelated Structures for a $V^{IV}O$ Species Formed by a Bidentate Ligand: (a) *cis*-Octahedral; (b) *trans*-Octahedral; and (c) Square Pyramidal

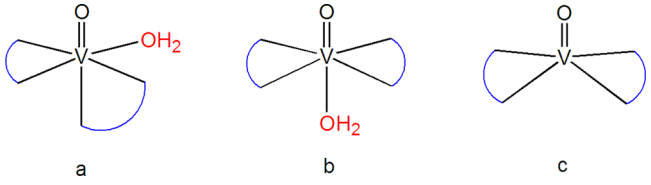

a b c

A search in the Cambridge Structural Database[48] for mononuclear oxidovanadium(IV) complexes formed by picolinate derivates yielded five structures. The two compounds synthesized by Gätjens et al.[19,20] with 5-carbomethoxypicolinic and 5-carboisopropoxypicolinic acid show *cis*-octahedral geometry (Scheme 2, a) with the two ligand anions in an (equatorial−equatorial) and (equatorial−axial) arrangement; in particular, two pyridine-N occupy the equatorial sites and the water molecule is in *trans* position to one of them to give the *OC*-6-24 isomer (Scheme 3). Orvig and co-workers proposed without the support of an X-ray determination the same arrangement for $[VO(pic)_2(H_2O)]$,[49] and this has been recently confirmed by some of us.[44d] A similar spatial arrangement was found also in the closely related species $[VO(imidazole\text{-}4\text{-}carboxylato)_2(H_2O)]$.[50] The third $V^{IV}O^{2+}$ complex is $[VO(6\text{-}ethylpicolinato)_2(H_2O)]$, which shows a *trans*-octahedral structure with the two ligands in the equatorial plane and the water *trans* to V=O (Scheme 2, b).[17] An analogous arrangement was found also for *trans*-$[VO(quinoline\text{-}2\text{-}carboxylato)_2(H_2O)]$, where the water molecule is coordinated in *trans* position to the V=O moiety.[51] The reason for the two different types of structure is the comparable stability of the possible isomers (*cis*-octahedral, *trans*-octahedral, and square pyramidal) for the bis-chelated species formed by picolinate derivatives;[44d] DFT calculations indicate that picolinate prefers the *cis*-octahedral arrangement, the *trans*-octahedral structure is favored if an alkyl substituent is in the 6 position of the ring (6-methylpicolinate, 6-ethylpicolinate), whereas the formation of a six-membered ring favors the square pyramidal geometry (2-pyridylacetate).[44d] The fourth and fifth X-ray structures were found in the system $V^{IV}O^{2+}/H_2$hypic: $[VO(Hhypic\text{-}N,O)(Hhypic\text{-}O,O')(H_2O)]$, with one ligand binding vanadium with pyridine-N and carboxylate-O and the other ligands with carboxylate-O and phenolate-O in a *cis*-octahedral arrangement,[18] and the cyclic tetramer $[(VO)_4(\mu\text{-}(hypic\text{-}N,O,O',O''))_4(H_2O)_4]$, with four bianionic ligands bound to vanadium and four carboxylate groups bridging the $V^{IV}O^{2+}$ units in a μ-1,3 mode.[18,52]

Concerning pyrazine-2-carboxylic acid, another search in the Cambridge Structural Database[48] revealed that only one mononuclear $V^{IV}O$ has been resolved through X-ray diffraction analysis.[53] Its formulation is $[VO(prz)_2(H_2O)]$ (isomer *OC*-6-24) with a *cis*-octahedral geometry and the two ligands assuming an (equatorial−equatorial) and an (equatorial−axial) arrangement, two pyrazine-N, a carboxylate-O, and a water molecule (*trans* to the nitrogen donor) in the equatorial position, and an axial carboxylate-O *trans* to the V=O group.[53]

Rather surprisingly, in this study the never seen before isomer *OC*-6-23 (**1**·2H_2O) as well as the known type *OC*-6-24 (**2**·4H_2O) were revealed for 5-cyanopyridine-2-carboxylic acid, whereas the structures of the isomer *OC*-6-24 were solved for 3-hydroxypyridine-2-carboxylic and pyrazine-2-carboxylic acid (**4**, **5**).

2. Synthesis and IR Characterization. $[VO(picCN)_2(H_2O)]\cdot 2H_2O$ (**1**·2H_2O), $[VO(picCN)_2(H_2O)]\cdot 4H_2O$ (**2**·4H_2O), $[VO(picFF)_2(H_2O)]$ (**3**), and $[VO(prz)_2(H_2O)]$ (**5**) were synthesized from $VOSO_4\cdot 5H_2O$ and

dx.doi.org/10.1021/ic500766t | Inorg. Chem. 2014, 53, 7960−7976

Scheme 3. Structure of the Four Possible Isomers of *cis*-Octahedral $V^{IV}O$ Complexes Formed by Picolinato and Pyrazine Derivatives and Their Configuration Indexes[a]

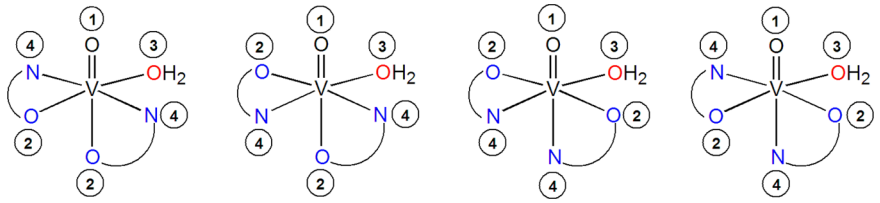

[a]According to ref 47, the configuration index of octahedral (*OC*-6) complexes consists of two digits: the first digit is the priority number of the ligating atom *trans* to the ligating atom of priority number 1, and the second digit of the configuration index is the priority number of the ligating atom *trans* to the most preferred ligand in the plane that is perpendicular to the reference axis (if there is more than one of the highest priority ligand in the plane, the priority number of the *trans* ligand having the largest numerical value is selected). The procedure for assigning priority numbers to the donor atoms is based upon the standard sequence rules developed for chiral carbon compounds by Cahn, Ingold, and Prelog (CIP rules).

a deprotonated picolinic or pyrazine derivative in a 1:2 ratio in a methanol/water solution. In the initial synthetic procedure $CH_3COONa·3H_2O$ was used as a base for all the systems, but the main disadvantage of this approach was the contamination of the products by sodium sulfate, in some cases observed even after repeated recrystallizations. Calcium acetate hydrate was found to be a suitable base to overcome this problem, and products in pure form were obtained. The previously reported synthetic procedure for compound **5**, starting from V_2O_5, V powder, and pyrazine-2-carboxylic acid under hydrothermal conditions, gave only a 9% yield.[53] Under our conditions, **5** was obtained in a 57% yield.

With 3-hydroxypyridine-2-carboxylic acid, $Na[VO(Hhypic)_3]·H_2O$ (**4**) was synthesized and characterized through X-ray diffraction analysis. With respect to the structures reported in the literature, in which the metal to ligand ratio was 1:1 and 1:2,[18,52] we were interested in obtaining an additional compound with the use of a larger amount of ligand, e.g., 1:3, and investigated this possibility using $CH_3COONa·3H_2O$ as a base. With this approach, the compound **4** was obtained as the only product.

IR spectroscopy shows the presence of water in all compounds **1**−**5**. The characteristic absorption band for the cyano group in **1** is observed at 2243 cm^{-1}. The differences between the asymmetrical (ν_{as}) and symmetrical (ν_s) stretching vibrations of the carboxylate groups in complexes **1**−**5** are in the range 196−263 cm^{-1}, indicating a monodentate coordination to the V═O moiety.[54] The characteristic absorption of the V═O stretching was observed between 981 and 967 cm^{-1}, which is consistent with six-coordinated vanadium species.[55] These results are in good agreement with the X-ray structural analysis (see below).

3. Description of the Solid Structures. *a. (OC-6-23)-[VO(picCN)$_2$(H$_2$O)]·2H$_2$O (**1**·2H$_2$O) and (OC-6-24)-[VO(picCN)$_2$(H$_2$O)]·4H$_2$O (**2**·4H$_2$O).* X-ray structural analysis showed that **1**·2H_2O crystallized in the triclinic $P\bar{1}$ space group as a racemate. The asymmetric unit contains one complex enantiomer and two additional water molecules. The structure of the complex is presented in Figure 1. Selected bond lengths (Å) and angles (deg) are summarized in Table 1. Compound **1** has a distorted octahedral geometry (Scheme 2, a) with two bidentate 5-cyanopyridine-2-carboxylate ligands (picCN) and one water molecule coordinated to the oxidovanadium moiety.

In **1** the equatorial positions are occupied by O2 and N1 of the first picCN ligand, pyridine N2 of the second ligand, and a water molecule, while axial positions are occupied by apical oxido O1 and carboxylate oxygen O4. The ligand in the (equatorial−equatorial) position is coordinated in such a way to have its carboxylate oxygen O2 in *trans* position to the water [O2−V1−O6 = 164.50(7)°] and the pyridine nitrogen atom N1 in *trans* position to N2 [N1−V1−N2 = 159.38(7)°]. Therefore, the isomer formed is *OC*-6-23. To the best of our knowledge, the structure of **1** is the first example of an *OC*-6-23 arrangement for bis(picolinato) $V^{IV}O$ complexes. The V−O

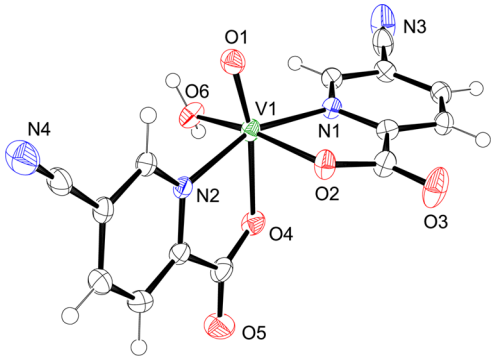

Figure 1. Structure of **1** with crystallographic numbering. Thermal ellipsoids are shown at the 50% probability level at 150 K.

Table 1. Selected Bond Distances and Angles for 1·2H$_2$O, 2·4H$_2$O, 4, and 5

	1·2H$_2$O	2·4H$_2$O	4	Λ-5
		Distances (Å)		
V1−O1	1.6004(16)	1.5956(16)	1.6015(18)	1.5888(15)
V1−O2	1.9955(15)	1.9681(16)	1.9984(19)	1.9798(15)
V1−O4	2.1162(16)	2.1390(16)	2.1581(18)	2.1485(14)
V1−O6	1.9884(16)	2.0114(17)	1.9810(19)	2.0373(15)
V1−N1	2.1246(17)	2.1230(19)	2.143(2)	2.1196(18)
V1−N2	2.1160(18)	2.1515(19)	2.139(2)	2.1462(15)
		Angles (deg)		
O1−V1−O2	100.05(8)	108.67(8)	107.90(10)	109.67(8)
O1−V1−O4	167.42(7)	162.92(8)	167.41(9)	166.42(7)
O1−V1−O6	94.73(8)	99.76(8)	101.89(9)	95.88(7)
O1−V1−N1	104.55(8)	95.17(8)	93.89(9)	97.52(8)
O1−V1−N2	92.63(7)	89.47(8)	94.35(9)	92.15(7)
O2−V1−O6	164.50(7)	87.26(7)	84.06(8)	91.11(6)
O6−V1−N1	93.53(7)	162.04(7)	159.72(9)	165.53(7)
N1−V1−N2	159.38(7)	97.58(7)	96.34(9)	90.80(6)

dx.doi.org/10.1021/ic500766t | *Inorg. Chem.* 2014, 53, 7960−7976

single bonds are 1.9884(16)−2.1162(16) Å, and the V−N bonds are 2.1160(18) and 2.1246(17) Å.

The presence of coordinated and noncoordinated water molecules in **1**·2H_2O enables the formation of several hydrogen bonds that connect molecules into infinite double layers parallel to the *ab* plane (Figure S1 of the Supporting Information). These layers are further connected into a 3D network by weak C−H···O/N interactions (Table S3), and the crystal lattice is additionally stabilized by $\pi\cdots\pi$ stacking (Table S4).

When **1**·2H_2O was recrystallized from a water solution at room temperature by slow evaporation of the solvents, crystals of **2**·4H_2O were obtained together with those of **1**·2H_2O. Also, when reaction conditions were modified and the reaction was performed at room temperature with a short reaction time and $CH_3COONa\cdot3H_2O$ was used instead of $Ca(CH_3COO)_2\cdot H_2O$, we were able to obtain crystals containing higher proportion of **2**·4H_2O, but **1**·2H_2O was still present. However, **2**·4H_2O quickly dehydrates outside the solution, and an amorphous solid is formed. The compound **2**·4H_2O also crystallized in the triclinic $P\bar{1}$ space group as a racemic mixture. In the asymmetric unit, besides one complex, four additional water molecules are included. Two of the noncoordinated water molecules are highly disordered. Compound **2** has a distorted octahedral geometry similar to compound **1**; however, the difference between the complexes is in the orientation of the equatorial picCN ligand. The carboxylate oxygen O2 in **2** occupies the binding site *cis* to the water molecule [O2−V1−O6 = 87.26(7)°], and the pyridine nitrogen N1 lies *cis* with respect to the pyridine N2 of the second ligand [N1−V1−N2 = 97.58(7)°]. The isomer formed is *OC*-6-24, and its structure is presented in Figure 2. Selected bond lengths (Å) and angles

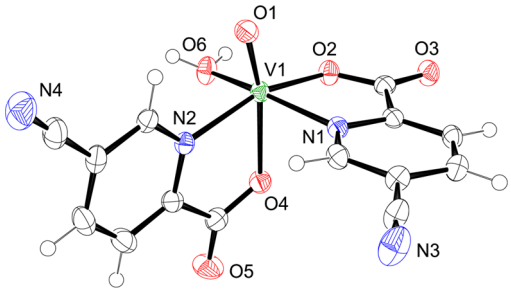

Figure 2. Structure of **2** with crystallographic numbering. Thermal ellipsoids are shown at the 50% probability level at 150 K.

(deg) are summarized in Table 1. This arrangement is analogous to that previously reported for oxidovanadium(IV) complexes with picolinate derivatives.[19,20] The V−O single bonds are 1.9681(16)−2.1390(16) Å, and the V−N bonds are 2.1230(19) and 2.1515(19) Å.

The crystal lattice of **2**·4H_2O is stabilized by a network of hydrogen bonds, as well as weak C−H···O/N interactions listed in Table S6 of the Supporting Information. Hydrogen bonds, which are observed between water molecules and heteroatoms of the complex or between different water molecules, form infinite double layers parallel to the *ab* plane similarly to that in structure **1**·2H_2O (Figure S2). Complexes are directly connected only through weak C3−H3···O1 and C6−H6···N3 interactions. No $\pi\cdots\pi$ stacking has been observed in this structure.

*b. (OC-6-24)-Na[VO(Hhypic)$_3$]·H_2O (**4**).* Compound **4** crystallized in the triclinic $P\bar{1}$ space group as a one-dimensional coordination polymer. The structure of the asymmetric unit is presented in Figure 3, whereas selected bond lengths (Å) and

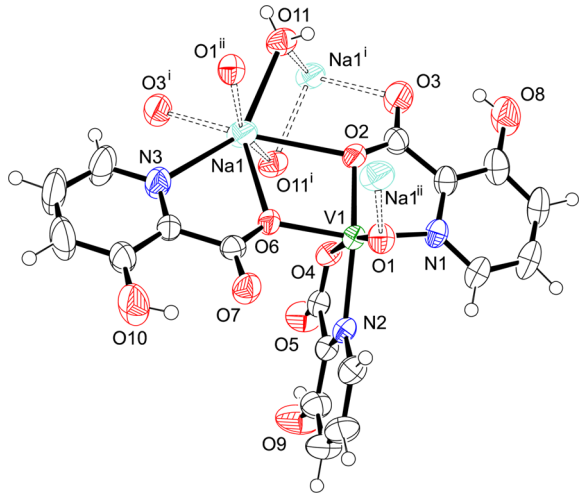

Figure 3. View of the asymmetric unit of compound **4** with crystallographic numbering. Thermal ellipsoids are shown at the 50% probability level at 293 K. Symmetry codes: (i) $-x, -y + 1, -z$; (ii) $-x + 1, -y + 1, -z$.

angles (deg) are summarized in Table 1. The asymmetric unit consists of a distorted oxidovanadium(IV) octahedral complex anion with three ligands, a sodium cation Na1, which is bridged to V1 through the O2, O6, and N3 atoms, and a water molecule coordinated to Na1. The ligands are in their monoanionic form with the phenolic group protonated; for this reason, they must be indicated with Hhypic(−).

The octahedral coordination sphere of the vanadium center in **4** is different from that formed in the other oxidovanadium(IV) complexes with H_2hypic.[18,52] In known mononuclear [VO(Hhypic-*N*,*O*)(Hhypic-*O*,*O*′)(H_2O)] the equatorial binding sites are occupied by carboxylate and phenolate oxygen atoms of one Hhypic(−) ligand, a pyridine nitrogen of the second Hhypic(−) ligand, and a water molecule, which is in *trans* position to carboxylate.[18] A similar arrangement of hypic(2−) ligands was found in the cyclic tetramer [$(VO)_4$(μ-(hypic-*N*,*O*,*O*′,*O*′′))$_4$($(H_2O)_4$].[18,52] In contrast, the arrangements and binding modes of the (equatorial−equatorial) and the (equatorial−axial) Hhypic(−) ligands in **4** are similar to those in **2** and **5**. The first ligand in **4** is coordinated bidentately by equatorial carboxylate O2 and pyridine N1 atoms, the second is coordinated bidentately by equatorial pyridine N2 and axial carboxylate O4, and the third one is coordinated monodentately by carboxylate O6 in *cis* position with respect to carboxylate O2 [O2−V1−O6 = 84.06(8)°] and is replacing water on the fourth equatorial site. The V−O single bonds are 1.9810(19)−2.1581(18) Å, and the V−N bonds are 2.139(2) and 2.143(2) Å. Interestingly, phenol groups in **4** are not deprotonated and therefore do not act as binding sites. This may result from the use of $CH_3COONa\cdot3H_2O$ in our case, which is a weaker base than $NaHCO_3$[18] or NaOH[52] used in previously published syntheses.

The presence of a sodium cation with high coordination number (seven) provides an interesting bridging network. Two asymmetric units, built from a vanadium complex anion, a sodium cation, and a water molecule, are bridged through the inversion center (Figure S3 of the Supporting Information). The O2, O6, and N3 atoms of the vanadium complex are

dx.doi.org/10.1021/ic500766t | Inorg. Chem. 2014, 53, 7960−7976

coordinated to the sodium ion, which is further connected to two adjacent vanadium complexes through the oxido O1($-x$ + 1, $-y$ + 1, $-z$) atom and carbonyl O3($-x$, $-y$ + 1, $-z$) atom and to an adjacent sodium ion by two symmetry-related bridging water molecules (O11, O11($-x$, $-y$ + 1, $-z$)), thus forming an infinite coordination polymer chain along the *a* axis (Figure S4 of the Supporting Information). Na−O and Na−N bond lengths are between 2.403(3) and 2.765(3) Å and are within the range found for other anionic vanadium complexes.[56]

The crystal lattice of **4** is stabilized by several hydrogen bonds, as well as weak C−H···O interactions listed in Table S8 of the Supporting Information. Hydrogen bonds O−H···O are formed only along the coordination polymer chain. The coordinated water participates in the stabilization of the chain structure through hydrogen bonds, while phenol groups participate only in the intraligand hydrogen bonds (Figure S4). Weak C−H···O as well as $\pi\cdots\pi$ stacking interactions have been found along the coordination polymer chain and also between different polymer chains (Table S9).

*c. (OC-6-24)-[VO(prz)$_2$(H$_2$O)] (Λ-**5**) and (OC-6-24)-[VO(prz)$_2$(H$_2$O)] (Δ-**5**).* Compound **5** crystallized in the chiral monoclinic $P2_1$ space group. One monocrystal contains one enantiomer. In our batch, we found crystals of both chiralities and were thus able to determine crystal structures of both Λ- and Δ-enantiomers. In the previously reported structure compound **5** crystallized under hydrothermal conditions as a dihydrate, [VO(prz)$_2$(H$_2$O)]·2H$_2$O (isomer *OC*-6-24) (yield = 9%), in the achiral monoclinic $P2_1/c$ space group as a racemic mixture of both enantiomers additionally containing two noncoordinated water molecules in the asymmetric unit.[53] We repeated the crystallizations under atmospheric conditions several times, and only crystals of Λ-**5** and Δ-**5** have been obtained. It seems that the formation of the dihydrate predominates only under hydrothermal conditions.

Since the geometrical parameters of Λ-**5** and Δ-**5** are almost identical, only the structure of Λ-**5** will be discussed. Selected bond lengths (Å) and angles (deg) for Λ-**5** are summarized in Table 1, and its structure is presented in Figure 4. Structural

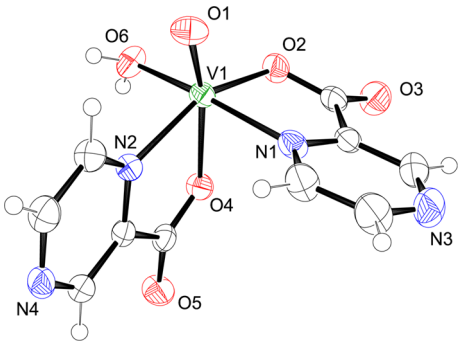

Figure 4. Structure of the Λ-enantiomer of **5** (Λ-**5**) with crystallographic numbering. Thermal ellipsoids are shown at the 50% probability level at 293 K.

details for Δ-**5** are reported in Tables S12 and S13 of the Supporting Information, whereas the structure is shown in Figure S6. Compound **5** has a distorted octahedral geometry with two bidentate pyrazine-2-carboxylate (prz) ligands coordinated to an oxidovanadium moiety and a water molecule at the equatorial site. Arrangement of the ligands is equal to the structure of **2**; that is, the isomer formed is *OC*-6-24. The V1−O/N distances of **5** are almost identical to the distances in the previously published dihydrate.[53]

Hydrogen bonding between coordinated water and heteroatoms causes the formation of a wavy plane, where complexes are connected along the *b* axis by an O6−H6*A*···N4 hydrogen bond, while O6−H6*B*···O5 hydrogen bonding is spreading the network along the *a* axis (Figure S5 of the Supporting Information). Additionally, the crystal structure of **5** is further stabilized by a weak C−H···O interaction (Table S11). No $\pi\cdots\pi$ stacking has been observed in this structure.

4. EPR Characterization of the Solid Structures. The isomer *OC*-6-23 of the solid compound **1** was dissolved in MeOH or DMF, in order to establish the geometry and the coordination mode of the ligands through EPR spectroscopy. Anisotropic spectra exhibit axial symmetry with two *g* and two *A* values. It has been recently demonstrated by DFT methods that the *x,y* anisotropy, expressed by the $|A_x - A_y|$ value, follows this order: $|A_x - A_y|$ (*trans*-octahedral) > $|A_x - A_y|$ (square pyramidal) > $|A_x - A_y|$ (*cis*-octahedral).[44d] Therefore, $|A_x - A_y|$ can be related to the geometry of the V^{IV}O species in solution. The low value of $|A_x - A_y|$ for **1**, not measurable for the large linewidth of the EPR absorptions in the perpendicular region, indicates that it maintains its *cis*-octahedral geometry in the organic solvent, with a water (or a MeOH/DMF molecule, if H$_2$O is replaced by the solvent) occupying the equatorial position. EPR parameters of this species (**I** in Figure 5) are g_z =

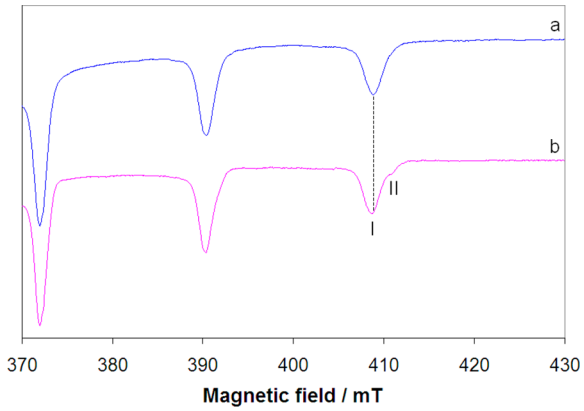

Figure 5. High-field region of the X-band anisotropic EPR spectra recorded at 120 K on [VO(picCN)$_2$(H$_2$O)] (**1**, isomer *OC*-6-23) dissolved in MeOH (a) and DMF (b). With **I** are indicated the M_I = 7/2 resonances of the isomer *OC*-6-23 or *OC*-6-24 of **1** and with **II** those of *OC*-6-42.

1.946 and $A_z = 164.5 \times 10^{-4}$ cm^{-1} in MeOH and g_z = 1.945 and $A_z = 163.7 \times 10^{-4}$ cm^{-1} in DMF. The value of ^{51}V A_z is similar to that measured for the isomer *OC*-6-24 formed by picolinate ([VO(pic)$_2$(H$_2$O)]) species.[44d,57−59] From EPR spectra, it is not possible to establish if the isomer *OC*-6-23 converts to *OC*-6-24 (**2**) (see Scheme 3) with the water in *trans* position to one of the two pyridine-N instead of the carboxylate-O because the additivity relationship[60] predicts the same values of A_z for the two species. To clarify this point, DFT simulations were carried out to calculate ^{51}V hyperfine coupling tensor ***A*** for the four possible *cis*-octahedral isomers of [VOL$_2$(H$_2$O)], with L = picCN, picFF, and prz. Using the half-and-half hybrid functional BHandHLYP and the basis set 6-311G(d,p), it is possible to calculate A_z with a percent deviation below 3% from the experimental value.[44e,61] The values calculated for A_x, A_y,

dx.doi.org/10.1021/ic500766t | Inorg. Chem. 2014, 53, 7960−7976

and A_z and the comparison with experimental A_z are given in Table 2.

Table 2. Calculated A_x, A_y, and A_z Values and Comparison with the Experimental A_z of the Isomers *OC*-6-23, *OC*-6-24, *OC*-6-42, and *OC*-6-44 for the Species $[VOL_2(H_2O)]$ Formed by picCN, picFF, and prz

ligand	isomer	A_x^{calcd}[a]	A_y^{calcd}[a]	A_z^{calcd}[a]	A_z^{exptl}[a]	dev %[b]
picCN	*OC*-6-24	−66.8	−62.0	−164.1	−165.3	−0.7
picCN	*OC*-6-23	−66.2	−62.8	−165.0	−165.3	−0.2
picCN	*OC*-6-42	−65.3	−63.0	−165.1	−169.3	−2.5
picCN	*OC*-6-44	−60.2	−52.6	−157.7	−169.3	−6.9
picFF	*OC*-6-24	−65.9	−62.5	−164.3	−164.8	−0.3
picFF	*OC*-6-23	−66.3	−62.7	−164.8	−164.8	0.0
picFF	*OC*-6-42	−65.4	−63.3	−165.5	−168.8	−1.9
picFF	*OC*-6-44	−57.5	−48.9	−154.2	−168.8	−8.7
prz	*OC*-6-24	−65.2	−62.7	−163.9	−164.0	−0.1
prz	*OC*-6-23	−66.2	−62.5	−164.7	−164.0	0.4
prz	*OC*-6-42	−65.2	−63.1	−165.3	−170.0	−2.8
prz	*OC*-6-44	−59.1	−51.0	−156.2	−170.0	−8.1

[a]Values reported in 10^{-4} cm^{-1}. [b]Percent deviation from the experimental A_z value calculated as $100 \times [(|A_z|^{calcd} - |A_z|^{exptl})/|A_z|^{exptl}]$.

DFT calculations confirm that two close values of A_z are expected for the isomers *OC*-6-23 and *OC*-6-24 (percent deviation of −0.2% and −0.7%). This should suggest that *OC*-6-23 maintains in solution its identity, even if it is not possible to rule out unambiguously the interconversion of *OC*-6-23 in *OC*-6-24 (the two species have comparable stability; see below). The structures of *OC*-6-23 and *OC*-6-24 are presented in Scheme 4, a and b.

In DMF a minor species is observable with $g_z = 1.943$ and $A_z = 169.5 \times 10^{-4}$ cm^{-1} (**II** in Figure 5). This complex may be the isomer of **1** with two carboxylate groups in the equatorial plane and one of the two pyridine-N in *trans* position to V═O, *OC*-6-42, or *OC*-6-44 (Scheme 3). The increase of A_z is due to the replacement of the aromatic nitrogen by a carboxylate-O, as expected by the additivity relationship.[60] The results reported in Table 2 indicate that *OC*-6-42, in contrast to *OC*-6-44, should give a value of A_z in agreement with the experiment; the percent deviation predicted in the two cases is −2.5% and −6.9%. The simulations of the relative stability of the two isomers confirm that *OC*-6-42 (Scheme 4, c) is significantly more stable than *OC*-6-44.

EPR spectra of $[VO(picFF)_2(H_2O)]$ (**3**) dissolved in MeOH and DMF are shown in Figure S7 of the Supporting Information. Of course, **3** can form any of the four *cis*-octahedral isomers represented in Scheme 3. In both the solvents two sets of resonances appear, the first (**I** in Figure S7) with $g_z = 1.944$ and $A_z = 164.1 \times 10^{-4}$ cm^{-1} (MeOH) and $g_z = 1.944$ and $A_z = 164.7 \times 10^{-4}$ (DMF) and the second one (**II** in Figure S7) with $g_z = 1.944$ and $A_z = 168.9 \times 10^{-4}$ cm^{-1} (MeOH) and $g_z = 1.944$ and $A_z = 168.1 \times 10^{-4}$ (DMF). These values are comparable with those measured for *OC*-6-23 and *OC*-6-42 isomers of $[VO(picCN)_2(H_2O)]$ (see above). DFT simulations for **3** (Table 2) indicate that the two isomers with two equatorial pyridine-N (*OC*-6-23 and *OC*-6-24) should have A_z values in the range $(164.3-164.8) \times 10^{-4}$ cm^{-1}, whereas the isomers with two carboxylate-O in the equatorial plane (*OC*-6-42 and *OC*-6-44) should be characterized by 165.5 and 154.2×10^{-4} cm^{-1}. Therefore, signals indicated by **I** in Figure S7 can be attributed to *OC*-6-24 or *OC*-6-23 species, whereas those indicated by **II** to *OC*-6-42. Their structures are represented in Scheme S1. It can be observed that the relative amount of *OC*-6-42 isomer with respect to *OC*-6-24/*OC*-6-23 is larger for picFF than picCN. This can be attributed to a better solvation of the complexes due to the presence of two electronegative F atoms.

The polycrystalline powder of $Na[VO(Hhypic)_3]\cdot H_2O$ (**4**) was dissolved in DMF and MeOH, and anisotropic EPR spectra were recorded (Figure S8 of the Supporting Information). As mentioned above, **4** differs from the structures reported in the literature for $V^{IV}O$−3-hydroxypyridine-2-carboxylate complexes because there are three instead of two ligands in the V coordination environment (see above). In this case, one species was detected in DMF (**I** in Figure S8) and two species were revealed in MeOH (**I** and **II** in Figure S8). **I** is characterized by $g_z = 1.948$ and $A_z = 164.7 \times 10^{-4}$ cm^{-1} (DMF) and $g_z = 1.947$ and $A_z = 164.8 \times 10^{-4}$ cm^{-1} (MeOH). These parameters are comparable with those of the complexes formed by picCN and picFF and are compatible with both isomers *OC*-6-24 and *OC*-6-23. This indicates that in a coordinating solvent the weak monodentate carboxylate group is replaced by a solvent molecule, even if the position of the solvent, *trans* to pyridine-N or to carboxylate-O, remains elusive. In MeOH the resonances of a second species appear, with $g_z = 1.942$ and $A_z = 169.6 \times 10^{-4}$ cm^{-1}; these values are similar to those of the *OC*-6-42 isomer of $[VO(picCN)_2(S)]$ and $[VO(picFF)_2(S)]$ (see Schemes 4 and S1). The possible structures of the three isomers of $[VO(Hhypic)_2(S)]$ are shown in Scheme S2 of the Supporting Information.

EPR characterization of $[VO(prz)_2(H_2O)]$ (**5**) was reported in the literature some years ago.[62] In this study, the spectra of **5** in DMF and MeOH were measured again. The resonances were attributed to the isomers *OC*-6-24 or *OC*-6-23 (**I** in Figure S9 of the Supporting Information) and *OC*-6-42 (**II** in Figure S9). The *cis*-octahedral arrangement of the two species is confirmed by the detection of a tetragonal spectrum, with a low value of the $|A_x - A_y|$ parameter. The relative amount of *OC*-6-42 with respect to *OC*-6-24/*OC*-6-23 is slightly higher in DMF than in MeOH. In DMF $g_z = 1.946$ and $A_z = 162.9 \times 10^{-4}$ cm^{-1}

Scheme 4. Structure of the Isomers of $[VO(picCN)_2(H_2O)]$ (1) in Solution: (a) *OC*-6-23; (b) *OC*-6-24; and (c) *OC*-6-42[a]

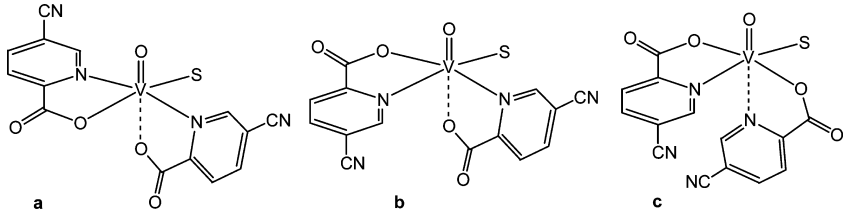

[a]S is a solvent molecule, H_2O or MeOH/DMF.

dx.doi.org/10.1021/ic500766t | Inorg. Chem. 2014, 53, 7960−7976

(*OC*-6-24/*OC*-6-23) and g_z = 1.945 and A_z = 169.0 × 10^{-4} cm^{-1} (*OC*-6-42) were measured, whereas in MeOH g_z = 1.946 and A_z = 163.6 × 10^{-4} cm^{-1} (*OC*-6-24/*OC*-6-23) and g_z = 1.945 and A_z = 169.3 × 10^{-4} cm^{-1} (*OC*-6-42) were obtained.

5. Behavior and Relative Stability of the *cis*-Octahedral Structures in Aqueous Solution. The behavior of the binary systems formed by $V^{IV}O^{2+}$ with HpicCN and HpicFF in aqueous solution has been studied as a function of the ligand to metal molar ratio and pH. The study of the systems with H_2hypic and Hprz has been already reported in the literature.[57,62] The protonation constants of the ligands and stability constants (log β_{pqr}) of the $V^{IV}O^{2+}$ complexes are listed in Table 3.

Table 3. Protonation Constants of the Ligands (HL or H_2L) and Stability Constants (log β_{pqr}) of the $V^{IV}O^{2+}$ Complexes at 25.0 ± 0.1 °C and *I* = 0.20 (KCl)[a]

species[b]	HpicCN	HpicFF	H_2hypic	Hprz
H_3L			16.99	5.56
H_2L	4.66(5)	4.43(14)	15.99	4.56
HL	2.95(1)	2.83(1)	10.91	2.73
VOLH			17.27	
VOL	4.16(6)	4.01(6)		3.42
VOL_2H_2			33.93	
VOL_2H			28.31	
VOL_2	7.44(2)	7.24(2)	20.50	6.09
VOL_2H_{-1}	1.37(11)	1.16(5)	10.03	–
$(VO)_2L_2H_{-2}$	1.78(3)	1.28(5)		0.11
$(VO)_4L_4$			66.70	
p*K* (VOL_2)	6.07	6.08	10.47	
ref	this work	this work	57	62

[a]The standard deviations (values of σ) are given in parentheses. [b]L indicates the fully deprotonated form of the ligand in water.

The distribution diagram of the species formed in the system $V^{IV}O^{2+}$/HpicCN with a metal to ligand molar ratio of 1:10 as a function of pH is shown in Figure 6; that with a metal to ligand ratio of 1:2 is reported in Figure S10 of the Supporting Information.

The fully protonated form of 5-cyanopyridine-2-carboxylic acid in aqueous solution is H_2L^+, with the protons on carboxylic and pyridinium groups, to which the values of pK_a of 1.71 and 2.95 are attributed. The electron-withdrawing effect of the

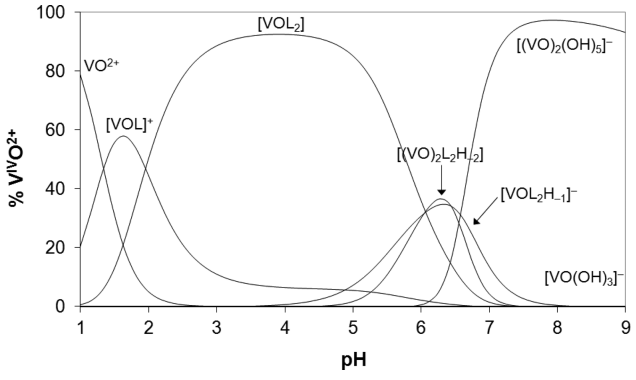

Figure 6. Distribution diagram of the species formed in the system $V^{IV}O^{2+}$/HpicCN (HL) as a function of pH with a total $V^{IV}O^{2+}$ concentration of 1.0 × 10^{-3} M and ligand to metal molar ratio of 1:10. L indicates the fully deprotonated form of the ligand in water.

−CN group lowers by more than 2 orders of magnitude the basicity of pyridine-N with respect to picolinic acid (5.19[57]). The pK_a of the carboxylic group is slightly higher than picolinic acid (1.71 vs ca. 1[57]). As it can be noticed from the examination of the distribution curves reported in Figure 6, picCN forms with $V^{IV}O^{2+}$ ion mono- and bis-chelated complexes in the pH range 1−7. The species VOL_2 undergoes deprotonation with a pK_a of 6.07 to give VOL_2H_{-1} (Table 3). This value is significantly lower than that expected for the deprotonation of a water molecule weakly bound in axial position and suggests the deprotonation of an equatorial water ligand; as a comparison, the pK_a measured for the analogous species of picolinate is 6.98.[57] The values of pK_a for the deprotonation of an equatorially coordinated water molecule in the species VOL_2 can vary from 4.75 for 1,10-phenanthroline[63] to 6.98 for picolinic acid,[57] 8.78 for maltol,[64] and 10.47−10.75 for pyridinones.[65]

EPR spectra recorded in aqueous solution with HpicCN are shown in Figure 7. From an examination of the spectra, it can

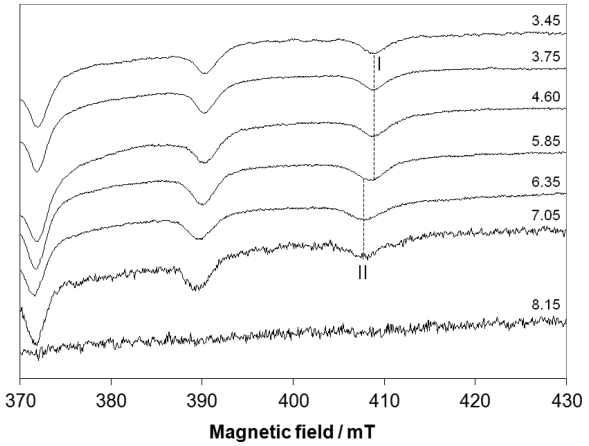

Figure 7. High-field region of the X-band anisotropic EPR spectra recorded at 120 K as a function of pH in the system $V^{IV}O^{2+}$/HpicCN with molar ratio 1:10 with a $V^{IV}O^{2+}$ concentration of 1.0 × 10^{-3} M. **I** indicates the M_I = 7/2 resonances of the isomer *OC*-6-23 or *OC*-6-24 of $[VO(picCN)_2(H_2O)]$ and **II** indicates those of *OC*-6-23 or *OC*-6-24 of $[VO(picCN)_2(OH)]^-$.

be observed that at this ligand to metal ratio $[VO(picCN)_2(H_2O)]$ is formed at acid pH values (**I** in Figure 7). This is due to the low basicity of the ligand, which undergoes deprotonation of the carboxylic group and pyridinium nitrogen with low pK_a values. EPR parameters are g_z = 1.946 and A_z = 165.3 × 10^{-4} cm^{-1}, comparable with those of the solid complex dissolved in MeOH or DMF and to $[VO(pic)_2(H_2O)]$.[57,58] From the additivity relationship and DFT calculations (see Table 2), however, it is not possible to establish if *OC*-6-24 or *OC*-6-23 exists or if, instead, a mixture of both of them is present in solution. For pH values higher than 6, the resonances of another species can be detected (**II** in Figure 7), to which the stoichiometry $[VOL_2H_{-1}]^-$ is assigned by potentiometry. This transformation is accompanied by a significant change of A_z values (A_z = 161.4 × 10^{-4} cm^{-1}) and can be clearly distinguished by EPR technique: in particular, on the basis of the additivity relationship, the replacement of a H_2O with a OH^- donor should reduce A_z by 4−5 × 10^{-4} cm^{-1}.[60]

dx.doi.org/10.1021/ic500766t | Inorg. Chem. 2014, 53, 7960−7976

Table 4. ΔG Values of Formation (in the Gas Phase and Aqueous Solution) and of Solvation for the Formation of the Isomers *OC*-6-23, *OC*-6-24, and *OC*-6-42 from *OC*-6-44 for the Species $[VOL_2(H_2O)]$ Formed by picCN, picFF, and prz[a,b]

		B3P86/6-311++G(d,p)			B3LYP/6-311++G(d,p)		
reaction	ligand	ΔG^{tot}_{gas}	$\Delta(\Delta G^{solv})$	ΔG^{tot}_{aq}	ΔG^{tot}_{gas}	$\Delta(\Delta G^{solv})$	ΔG^{tot}_{aq}
OC-6-44 ⇆ *OC*-6-23	picCN	−30.5	14.1	−16.4	−27.6	14.1	−13.5
OC-6-44 ⇆ *OC*-6-24	picCN	−32.1	13.0	−19.1	−27.5	13.7	−13.8
OC-6-44 ⇆ *OC*-6-42	picCN	−28.6	15.5	−13.1	−28.4	16.7	−11.7
OC-6-44 ⇆ *OC*-6-23	picFF	−44.2	28.7	−15.5	−34.3	28.8	−5.5
OC-6-44 ⇆ *OC*-6-24	picFF	−42.3	30.3	−12.0	−31.3	30.0	−1.3
OC-6-44 ⇆ *OC*-6-42	picFF	−44.1	29.5	−14.6	−37.9	35.6	−2.3
OC-6-44 ⇆ *OC*-6-23	prz	−32.4	18.0	−14.4	−29.2	18.1	−11.1
OC-6-44 ⇆ *OC*-6-24	prz	−33.3	18.4	−14.9	−38.6	18.8	−19.8
OC-6-44 ⇆ *OC*-6-42	prz	−32.9	22.7	−10.2	−32.8	22.7	−10.1

[a]Values reported in kJ mol^{-1}. [b]PCM model used with water as the solvent.

Above pH 8, stepwise displacement of the ligands by hydroxide ions results in the formation of dinuclear complex $[(VO)_2(OH)_5]^-$, which is EPR-silent.

In the fully protonated form in aqueous solution, 3,5-difluoropyridine-2-carboxylic acid can be indicated with H_2L^+, with the protons on pyridine N and the carboxylic group. The pK_a of such groups in the measured pH range are 1.60 (carboxylic) and 2.83 (pyridinium nitrogen). In the system $V^{IV}O^{2+}$/HpicFF, potentiometry suggests the presence of VOL, VOL_2, $(VO)_2L_2H_{-2}$, and VOL_2H_{-1} species. Analogously to the system with HpiCN, VOL_2 is formed at low pH value and deprotonates with a pK_a of 6.08 to give VOL_2H_{-1}; the dinuclear complex $(VO)_2L_2H_{-2}$ forms in low amount at a ligand to metal ratio of 10. Anisotropic EPR spectra recorded as a function of pH in the system $V^{IV}O^{2+}$/HpicFF with a molar ratio of 1:10 and $V^{IV}O^{2+}$ concentration of 1.0×10^{-3} M are shown in Figure S11 of the Supporting Information. As in the system with picCN, the complexation process starts at low pH values. The first species formed is $[VO(picFF)_2(H_2O)]$ (*OC*-6-24 or *OC*-6-23 isomer). The values of g_z and A_z are 1.945 and 164.8×10^{-4} cm^{-1}, very similar to those of the identical species formed in the solid state (g_z = 1.944 and A_z = 164.1−164.7 × 10^{-4} cm^{-1}; see **I** in Figure S11). However, an enlargement of the M_I = 7/2 resonance at higher magnetic field values indicates that a second complex is in equilibrium with it. Such a compound is characterized by g_z 1.945 and A_z 168.8×10^{-4} cm^{-1}, and these parameters are comparable with those of the *OC*-6-42 isomer (g_z = 1.944 and A_z = 168.1−168.9 × 10^{-4} cm^{-1}, **II** in Figure S11). Thus, the behavior in aqueous solution is similar to that of the solid sample dissolved in an organic solvent. It can be noticed that in the system with picCN the isomer *OC*-6-42 is not detected in water, in agreement with the fact that it is not revealed in MeOH and exists in low amount in DMF (Figure 5). With picFF, instead, the relative amount of *OC*-6-42 with respect to *OC*-6-24/*OC*-6-23 is significantly higher in organic solvents (see Figure S7 of the Supporting Information), and the same is observed in aqueous solution. In the pH range 5.5−6.5, the equatorial water molecule deprotonates and $[VO(picFF)_2(H_2O)]$ transforms into $[VO(picFF)_2(OH)]^-$ (**III** in Figure S11). At a pH higher than 8.5, the EPR signal disappears because of the formation of $V^{IV}O$ hydrolytic species.

The behavior in aqueous solution of the system $V^{IV}O^{2+}$/H_2hypic was investigated by Kiss et al.[57] The free ligand (H_3L^+ in its fully protonated form) is characterized by three pK_a values: pK_a ∼1 belongs to the carboxylic group, pK_a of 5.08 to pyridinium nitrogen, and pK_a of 10.91 to the phenolic group. Potentiometric and spectroscopic data suggested that, using a metal to ligand molar ratio of 1:3 and a $V^{IV}O^{2+}$ concentration of 1.0×10^{-3} M, at physiological pH three species exist in solution: $[VO(Hhypic)(hypic)]^-$, $[VO(hypic)_2]^{2-}$, and $[(VO)_4(\mu\text{-hypic})_4(H_2O)_4]$. On the basis of the thermodynamic stability constants 55.5%, 21.6%, and 22.0% of these species is expected in solution.[57] In $[VO(Hhypic)(hypic)]$ the two ligand molecules coordinate $V^{IV}O^{2+}$ with donor sets (N, COO^-) and (COO^-, O^-), and the EPR parameters are g_z = 1.943 and A_z = 167×10^{-4} cm^{-1}; in $[VO(hypic)_2]^{2-}$ the coordination mode becomes 2 × (COO^-, O^-) and the EPR parameters are g_z = 1.945 and A_z = 165×10^{-4} cm^{-1}; $[(VO)_4(\mu\text{-hypic})_4(H_2O)_4]$ is characterized by a broad absorption, superimposed to the signals due to the mononuclear complexes $[VO(Hhypic)(hypic)]^-$ and $[VO(hypic)_2]^{2-}$, indicating a significant interaction between the paramagnetic centers.[18b,57]

The binary system $V^{IV}O^{2+}$/Hprz has been recently studied by pH-potentiometric and spectroscopic measurements.[62] The results indicate the formation of $[VO(prz)(H_2O)_2]^+$, $[VO(prz)_2(H_2O)]$, and $[(VO)_2(prz)_2(OH)_2]$, which is favored in an equimolar solution at a high concentration of $V^{IV}O^{2+}$ ion. The pyrazine-2-carboxylate ligand forms five-membered chelate rings with the (N, COO^-) donor set. $[VO(prz)_2(H_2O)]$ exists as two isomers, i.e., *OC*-6-24 or *OC*-6-23 and *OC*-6-42 (Scheme 3); *OC*-6-24 is the same species observed in the solid state, whereas *OC*-6-42 is analogous to the compound formed with picCN and picFF. However, differently from the systems with picCN and picFF, $[VO(prz)_2(OH)]^-$ is not detected; probably it forms in a small amount and its formation coincides with that of the hydrolytic species $[(VO)_2(OH)_5]^-$ and $[VO(OH)_3]^-$.

The stability of the four possible *cis*-octahedral isomers can be evaluated calculating the free energy in the gas phase (G^{tot}_{gas}) or aqueous solution (G^{tot}_{aq}) (see Experimental and Computational Section). Therefore, the free energy for the formation of *OC*-6-23, *OC*-6-24, and *OC*-6-42 species from the less stable isomer, *OC*-6-44 (reactions *OC*-6-44 ⇆ *OC*-6-23, *OC*-6-44 ⇆ *OC*-6-24, *OC*-6-44 ⇆ *OC*-6-42), is

$$\Delta G^{tot}_{gas} = \Delta E^{ele} + \Delta G^{therm} \quad (1)$$

$$\Delta G^{tot}_{aq} = \Delta E^{ele} + \Delta G^{therm} + \Delta(\Delta G^{solv}) \quad (2)$$

The free energy in the gas phase and in aqueous solution was calculated at the B3P86/6-311++G(d,p) and B3LYP/6-311++G(d,p) levels of theory, and the solvent effect was computed with the PCM model.[45] Results are reported in Table 4 for picCN, picFF, and prz and allow us to determine the following conclusions: (i) it has been observed in the literature that only

dx.doi.org/10.1021/ic500766t | Inorg. Chem. 2014, 53, 7960−7976

a qualitative description can be obtained for these simulations,[66] and this is confirmed also by this study; (ii) B3P86 and B3LYP functionals give a comparable stability order between the four isomers and, generally, B3P86 suggests a higher stability of the three isomers *OC*-6-23, *OC*-6-24, and *OC*-6-42 with respect to *OC*-6-44; (iii) the stability of the two isomers with two pyridine-N in the equatorial plane (*OC*-6-23 and *OC*-6-24) is similar, and this does not allow us to establish which of them exists or if they coexist in aqueous solution (their EPR ^{51}V A_z values should be almost coincident; see Table 2); (iv) between the two isomers with two equatorial carboxylate-O (*OC*-6-42 and *OC*-6-44), *OC*-6-44 is the less stable, and this supports the experimental evidence (^{51}V A_z value calculated for *OC*-6-42 approaches the experimental one, whereas that of *OC*-6-44 is much lower than that observed). It can be supposed that the lower stability of *OC*-6-44 than *OC*-6-42 is due to the electrostatic repulsion of the two charged carboxylate groups in *cis* position (predicted O−V−O angles of 93.4° for the picCN isomer, 94.7° for picFF, and 93.8° for prz and predicted distance between O atoms of the two carboxylates of 2.83, 2.84, and 2.84 Å, respectively); (v) the stability order in the gas phase, beyond the numerical value, is the same as predicted in the aqueous solution.

Overall, on the basis of the DFT simulations, the more stable isomers are *OC*-6-23 and *OC*-6-24 for picCN (the two structures **1** and **2** solved by X-ray diffraction analysis), *OC*-6-24 for prz (the experimental X-ray structure **4**), and *OC*-6-23 for picFF (however, in the absence of an X-ray diffraction analysis, this should not be distinguishable from isomer *OC*-6-24 with EPR spectroscopy).

6. Interaction with the Blood Proteins. In the binary system $V^{IV}O^{2+}$/picolinate with a metal to ligand molar ratio of 1:2, vanadium is present in solution at physiological pH mainly as the complex $[VO(pic)_2(OH)]^-$ (isomer *OC*-6-24), while the bis-chelated $[VO(pic)_2(H_2O)]$ (*OC*-6-24) and the hydrolytic species $[(VO)_2(OH)_5]^-$ exist in smaller amounts; this was demonstrated by EPR and pH-potentiometric measurements.[57] The ternary systems with apo-hTf and holo-hTf show a very different behavior.[27c,d,i] In the system containing apo-hTf, $V^{IV}O^{2+}$ is bound to the iron sites to form (VO)(apo-hTf) and $(VO)_2$(apo-hTf), which are in equilibrium with the mixed complex (VO)(apo-hTf)(pic), in which picolinate, behaving as a synergistic anion,[67] replaces bicarbonate in the specific sites.[27c] This type of coordination is indicated by the shoulder appearing at lower magnetic fields with respect to the $M_I = 7/2$ resonance of (VO)(apo-hTf)/$(VO)_2$(apo-hTf).[27c]

In the system with HpicCN, EPR spectra were recorded with a ratio $V^{IV}O^{2+}$/HpicCN/apo-hTf of 2:4:1; therefore, in principle all $V^{IV}O^{2+}$ ions may be bound by picCN to form quantitatively $[VO(picCN)_2(H_2O)]$ or by apo-hTf to form $(VO)_2$(apo-hTf). In trace b of Figure 8, it can be observed that the spectrum is coincident with that of $(VO)_2$(apo-hTf);[27a] this means that picCN is a ligand not so strong to compete with apo-hTf for $V^{IV}O^{2+}$ coordination. No trace of $[VO(picCN)_2(H_2O)]$ or $[VO(picCN)_2(OH)]^-$ is observable at these experimental conditions. At the same experimental conditions, picolinate forms (VO)(apo-hTf)(pic) with apo-hTf with the coordination of $VO(pic)^+$ to the specific iron-binding sites,[27c,d] and $VO(pic)_2$(holo-hTf) with holo-hTf (*OC*-6-24 isomer with the equatorial binding of His-N) because the iron sites are occupied by Fe^{3+} ions.[27i] The different behavior of pic and picCN and the capability of picolinate to form mixed species can be related to the greater basicity of picolinic than 5-cyanopyridine-2-carboxylic acid (pK_a of the pyridinium group is 5.19 for Hpic[57] and 2.95 for HpicCN).

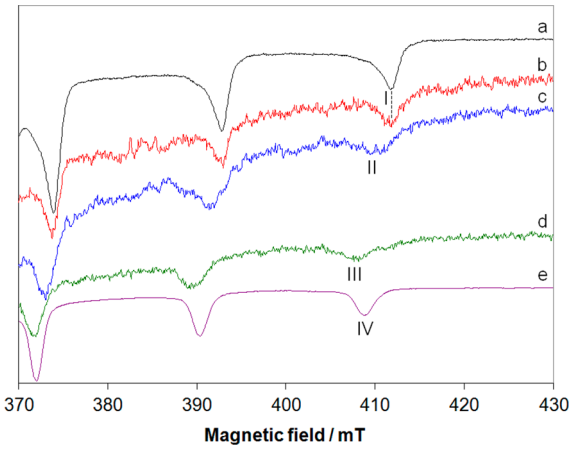

Figure 8. High-field region of the anisotropic X-band EPR spectra recorded at pH 7.40 on frozen solutions (120 K) containing (a) $V^{IV}O^{2+}$/apo-hTf 2:1 ($V^{IV}O^{2+}$ 5.0×10^{-4} M); (b) $V^{IV}O^{2+}$/HpicCN/apo-hTf 2:4:1 ($V^{IV}O^{2+}$ 5.0×10^{-4} M); (c) $V^{IV}O^{2+}$/HpicCN 1:2 ($V^{IV}O^{2+}$ 1.0×10^{-3} M); (d) $V^{IV}O^{2+}$/HpicCN 1:10 ($V^{IV}O^{2+}$ 1.0×10^{-3} M); and (e) $[VO(picCN)_2(H_2O)]$ (*OC*-6-23) dissolved in MeOH. **I**, **II**, **III**, and **IV** indicate the $M_I = 7/2$ resonances of $(VO)_2$(apo-hTf), $[VO(picCN)_2(H_2O)]$ (isomer *OC*-6-24 or *OC*-6-23), $[VO(picCN)_2(OH)]^-$ (isomer *OC*-6-24 or *OC*-6-23), and $[VO(picCN)_2(S)]$ (isomer *OC*-6-24 or *OC*-6-23).

The behavior of the system $V^{IV}O^{2+}$/HSA is significantly different when studied at different molar ratios. In particular, EPR spectra of an equimolar solution are characterized by the presence of the signals attributable to a dinuclear species, denoted as $(VO)_2$HSA, in which two $V^{IV}O^{2+}$ ions are magnetically coupled.[27a,b] When the metal to protein ratio is increased to 2:1 or higher, the EPR resonances are attributable to a multinuclear complex $(VO)_x$HSA (x = 5 or 6), in which the metal ions are not coupled and have similar coordination environments.[27a,b] Competition experiments between Zn^{2+} and $V^{IV}O^{2+}$ ions suggest that $V^{IV}O^{2+}$ has two types of binding sites, one of them corresponding to the multimetal binding site.[26b] The possible coordination at the specific site in the N-terminal region, where Cu^{2+} and Ni^{2+} are bound with the donor set (NH_2, N^-, N^-, N_{His}), has been ruled out on the basis of EPR evidence.[68]

The EPR spectrum measured in the ternary system $V^{IV}O^{2+}$/HpicCN/HSA 4:8:1 is shown in trace b of Figure S12 of the Supporting Information. It can be observed that it is different with respect to those recorded in the binary systems $V^{IV}O^{2+}$/HSA 4:1 and $V^{IV}O^{2+}$/HpicCN 1:2. This indicates that, besides $(VO)_x$HSA (**I** in Figure S12), at least two other species exist in solution (**II** and **III** in Figure S12). These species may be two mixed complexes with stoichiometry $VO(picCN)_2$(HSA) (isomer *OC*-6-23 or *OC*-6-24, **II**) and VO(picCN)(HSA)(H_2O) (**III**). To demonstrate the formation of $VO(picCN)_2$(HSA), EPR spectra of the system $V^{IV}O^{2+}$/HpicCN/1-MeIm 1:2:4 were recorded, because it was proved that 1-methylimidazole is a good model for His-N coordination;[25,27c,i] in this system $[VO(picCN)_2(1\text{-MeIm})]$ is formed, even if it is not possible to establish which of the two isomers *OC*-6-24 or *OC*-6-23 exists (or if they coexist). Therefore, $VO(picCN)_2$(HSA) is formed after the replacement of a water molecule by an accessible His-N (probably present on the protein surface; see Scheme 5, a). This has been already

dx.doi.org/10.1021/ic500766t | *Inorg. Chem.* 2014, 53, 7960−7976

Scheme 5. Structure of the Mixed Complexes Formed in the Ternary System $V^{IV}O^{2+}$/HpicCN/HSA: (a) $VO(picCN)_2(HSA)$ (Isomer *OC*-6-24), (b) $VO(picCN)_2(HSA)$ (Isomer *OC*-6-23), and (c) $VO(picCN)(HSA)(H_2O)$

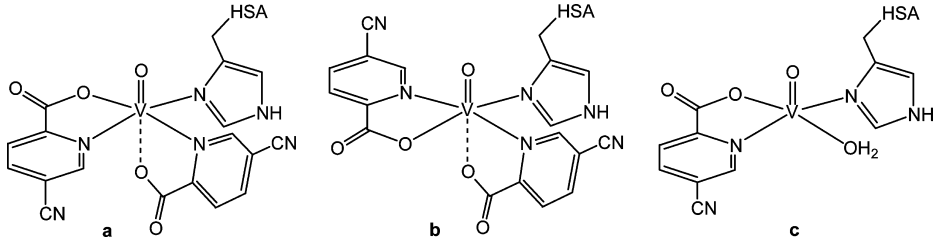

Table 5. Calculated A_x, A_y, and A_z Values and Comparison with Experimental A_z for $V^{IV}O$ Mixed Species Formed by picCN and prz with 1-MeIm and HSA

ligand	$A_x^{calcd a}$	$A_y^{calcd a}$	$A_z^{calcd a}$	$A_z^{exptl a,b}$	dev %[c]
$[VO(picCN)_2(1\text{-MeIm})]^d$	−57.2	−54.5	−155.9	−161.0	−3.2
$[VO(picCN)(1\text{-MeIm})(H_2O)]^+$	−67.0	−64.1	−168.8	−170.0	−0.7
$[VO(picCN)(1\text{-MeIm})(OH)]$	−48.3	−45.1	−148.5	−170.0	−12.6
$[VO(prz)_2(1\text{-MeIm})]^d$	−58.9	−55.8	−156.6	−160.6	−2.5
$[VO(prz)(1\text{-MeIm})(H_2O)]^+$	−66.4	−64.9	−168.8	−169.7	−0.5
$[VO(prz)(1\text{-MeIm})(OH)]$	−58.6	−55.9	−159.9	−169.7	−5.8

[a]Values reported in 10^{-4} cm^{-1}. [b]A_z^{exptl} of the species $VOL_2(HSA)$ and $VOL(HSA)(H_2O)$, with L = picCN, prz. [c]Percent deviation from the experimental A_z value calculated as $100 \times [(|A_z|^{calcd} - |A_z|^{exptl})/|A_z|^{exptl}]$. [d]The simulations were carried out on the isomer *OC*-6-24.

observed for other systems containing a VOL_2 species and albumin[25,27c,f,g] and is an unspecific binding mode displayed also by other proteins such as immunoglobulin G[27e] and hemoglobin.[69] Furthermore, EPR parameters of $VO(picCN)_2(HSA)$ (g_z = 1.947 and A_z = 161.0 × 10^{-4} cm^{-1}) are similar to those of the hydroxido species $[VO(picCN)_2(OH)]^-$ (*OC*-6-24 or *OC*-6-23), analogously to what is observed for picolinate mixed complex $VO(pic)_2(HSA)$.[27c] To prove the assignment of the resonances of species **I** to $VO(picCN)_2(HSA)$, DFT calculations at the BHandHLYP/6-311G(d,p) level of theory were carried out on $[VO(picCN)_2(1\text{-MeIm})]$ (we have chosen the isomer *OC*-6-24). The results are shown in Table 5 and indicate that, as expected, its ^{51}V A_z is similar to that of $VO(picCN)_2(HSA)$.

The species **II** may be a 1:1 species of picCN, stabilized by the binding of a His-N, $VO(picCN)(HSA)(H_2O)$ (Scheme 5, b). A similar compound has been proposed by Orvig's group in the system with maltol and has been detected also with 6-methylpicolinate,[25,27c] and it appears to be favored by a weak ligand. DFT calculations performed on $[VO(picCN)(1\text{-MeIm})(H_2O)]^+$ and on the species formed upon the deprotonation of a H_2O molecule, $[VO(picCN)(1\text{-MeIm})(OH)]$, confirm this assumption.

EPR spectra in the ternary system $V^{IV}O^{2+}$/HpicFF/apo-hTf were recorded at two different molar ratios, 2:4:1 and 4:8:1 (traces b and c of Figure 9). Furthermore, apo-hTf was added to $[VO(picFF)_2(H_2O)]$ at pH 6.70 (trace b) and 5.10 (trace c). The spectrum recorded at physiological pH in the $V^{IV}O^{2+}$/HpicFF system at 1:10 ratio is shown in trace d. The comparison between the spectra shows that only $(VO)_2$(apo-hTf) is formed. When the ratio $V^{IV}O^{2+}$/HpicFF/apo-hTf 2:4:1 is used, this is explainable postulating that all $V^{IV}O^{2+}$ in solution is complexed by apo-hTf. When the $V^{IV}O^{2+}$/HpicFF/apo-hTf ratio is brought to 4:8:1 ($V^{IV}O^{2+}$ 1.0 × 10^{-3} M), one may expect that 2.5 × 10^{-4} M hTf binds 5.0 × 10^{-4} M $V^{IV}O^{2+}$, whereas the rest of the $V^{IV}O^{2+}$ ions bind to picFF to form bis-chelated complexes. Instead, under these conditions, only $(VO)_2$(apo-hTf) is formed, and the excess of $V^{IV}O^{2+}$ (5.0 × 10^{-4} M) undergoes hydrolytic reactions, favored by low metal concentration. Of course, these results depend on the low strength of the ligand picFF.

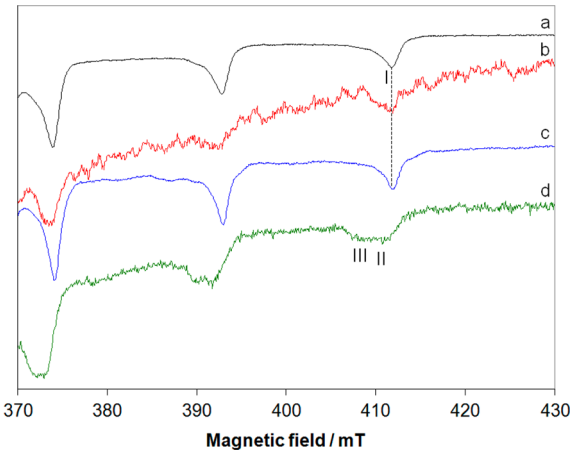

Figure 9. High-field region of the anisotropic X-band EPR spectra recorded at pH 7.40 on frozen solutions (120 K) containing (a) $V^{IV}O^{2+}$/apo-hTf 2:1 ($V^{IV}O^{2+}$ 5.0 × 10^{-4} M); (b) $V^{IV}O^{2+}$/HpicFF/apo-hTf 2:4:1 ($V^{IV}O^{2+}$ 5.0 × 10^{-4} M), hTf added at pH 6.70; (c) $V^{IV}O^{2+}$/HpicFF/apo-hTf 4:8:1 ($V^{IV}O^{2+}$ 1.0 × 10^{-3} M), hTf added at pH 5.10; and (d) $V^{IV}O^{2+}$/HpicFF 1:10 ($V^{IV}O^{2+}$ 1.0 × 10^{-3} M). **I**, **II**, and **III** indicate the M_I = 7/2 resonances of $(VO)_2$(apo-hTf), $[VO(picFF)_2(H_2O)]$ (isomer *OC*-6-24 or *OC*-6-23), and $[VO(picFF)_2(OH)]^-$ (isomer *OC*-6-24 or *OC*-6-23).

Another very important observation concerns the experiments when apo-hTf is added to $[VO(picFF)_2(H_2O)]$ at pH 6.70 or 5.10. It can be easily observed that in the first case the spectral signal is very weak, indicating that the amount of $(VO)_2$(apo-hTf) is significantly lower than that formed in the second case. It has been shown that, in the absence of Fe^{3+} coordination, transferrin assumes an "open conformation", so $V^{IV}O^{2+}$ coordination should not be influenced by the pH at which $[VO(picFF)_2(H_2O)]$ and protein are put in contact.[26c,27i] Therefore, the lower amount of $(VO)_2$(apo-hTf)

dx.doi.org/10.1021/ic500766t | Inorg. Chem. 2014, 53, 7960−7976

revealed at pH 6.70 can be related only to the formation of polynuclear, hydrolytic species of $V^{IV}O^{2+}$ ion (such as $[(VO)_2(OH)_5]^-$ and species with higher nuclearity), which hinder the binding to the specific sites of apo-hTf. This phenomenon appears to be important when the organic carrier is weak and the hydrolysis of $V^{IV}O^{2+}$ ion starts at a pH significantly lower than 7.40. In such situations, $V^{IV}O^{2+}$ cannot be sequestered by hTf and exists in solution as hydroxido complexes, which for their polynuclear structure cannot cross the cell membrane. For such compounds a low insulin-mimetic action is expected. In this context, however, it must be taken into account that the formation of polynuclear hydrolytic products should be significantly suppressed at the V concentrations necessary to observe insulin-enhancing effects, in the range 1−100 μM.[70]

The results in the system with HSA are comparable to those obtained with apo-hTf. The EPR spectrum measured in the ternary system $V^{IV}O^{2+}$/HpicFF/HSA 4:8:1 is superimposable with that recorded in the binary system $V^{IV}O^{2+}$/HSA 4:1 (traces a and b of Figure S13 of the Supporting Information). However, since the resonances of $[VO(picFF)_2(OH)]^-$ (*OC*-6-24 or *OC*-6-23) fall below those of $(VO)_x$(HSA) (cf. traces a and c), the presence of a low amount of $[VO(picFF)_2(OH)]^-$ (**III** in Figure S13) in solution cannot be ruled out completely. As for the system with apo-hTf, these results can be explained with the low basicity of picFF, which at the physiological conditions is not able to coordinate $V^{IV}O^{2+}$ ion.

In the binary system $V^{IV}O^{2+}/H_2$hypic 1:3, at physiological pH, $[VO(Hhypic)(hypic)]^-$, $[VO(hypic)_2]^{2-}$, and the tetranuclear species $[(VO)_4(\mu\text{-hypic})_4(H_2O)_4]$ exist (see above). The $M_I = 7/2$ resonances of the first two species are indicated by **II** and **III** in trace c of Figure 10, whereas the unresolved isotropic

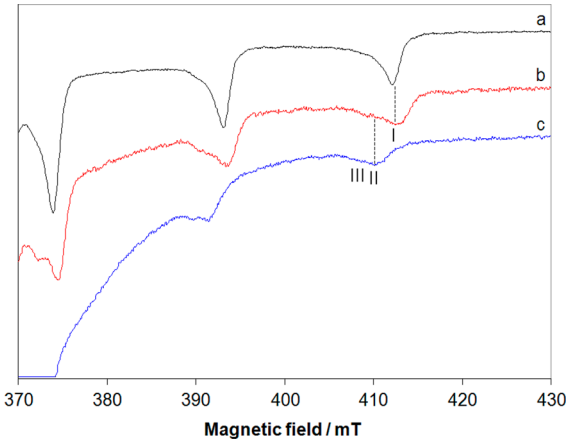

Figure 10. High-field region of the anisotropic X-band EPR spectra recorded at pH 7.40 on frozen solutions (120 K) containing (a) $V^{IV}O^{2+}$/apo-hTf 2:1 ($V^{IV}O^{2+}$ 5.0 × 10^{-4} M); (b) $V^{IV}O^{2+}/H_2$hypic/apo-hTf 2:6:1 ($V^{IV}O^{2+}$ 5.0 × 10^{-4} M); and (c) $V^{IV}O^{2+}/H_2$hypic 1:3 ($V^{IV}O^{2+}$ 1.0 × 10^{-3} M). **I**, **II**, and **III** indicate the resonances $M_I = 7/2$ of $(VO)_2$(apo-hTf), $[VO(Hhypic)(hypic)]^-$, and $[VO(hypic)_2]^{2-}$. The isotropic band is due to $[(VO)_4(\mu\text{-hypic})_4(H_2O)_4]$.

band below these signals is attributed to $[(VO)_4(\mu\text{-hypic})_4(H_2O)_4]$. The potentiometric and EPR results suggest that in solution the monodentate carboxylate group in the fourth equatorial position of $Na[VO(Hhypic)_3]$ (**4**) is replaced by water and that around physiological pH the salicylate-like coordination is favored (donor set (COO^-, O^-)). The behavior of the ternary system containing $V^{IV}O^{2+}$, apo-hTf, and H_2hypic differs considerably from that with HpicCN and HpicFF, where all $V^{IV}O^{2+}$ was complexed by transferrin due to the low strength of these ligands. The EPR spectrum recorded in the ternary system $V^{IV}O^{2+}/H_2$hypic/apo-hTf shows the presence of $(VO)_2$(apo-hTf) (**I** in Figure 10) as the main species and $[VO(Hhypic)(hypic)]^-$ and $[VO(hypic)_2]^{2-}$ (**II** and **III** in Figure 10) as minor ones. The relative amount between $(VO)_2$(apo-hTf) and $[VO(Hhypic)(hypic)]^-$ plus $[VO(hypic)_2]^{2-}$, calculated with the reported stability constants,[27d,57] is ca. 6:1. However, the large and isotropic absorption superimposed to the resonances of such species indicates the presence of $[(VO)_4(\mu\text{-hypic})_4(H_2O)_4]$, whose percentage cannot be determined exactly by EPR spectroscopy. The contemporaneous presence of the bis-chelated complexes of 3-hydroxypyridine-2-carboxylate, besides $(VO)_2$(apo-hTf), is due to the strength of hypic(2−) ligand.

The results obtained in the system $V^{IV}O^{2+}/H_2$hypic/HSA 4:12:1 are easily interpreted on the basis of the previous discussion. The EPR spectrum, shown in trace b of Figure S14 of the Supporting Information, shows the presence of more than one species. One of them is $(VO)_x$(HSA), which coexists at physiological pH with the two bis-chelated species $[VO(Hhypic)(hypic)]^-$ and $[VO(hypic)_2]^{2-}$ and with the tetranuclear complex $[(VO)_4(\mu\text{-hypic})_4(H_2O)_4]$, characterized by the peculiar broad absorption.[18b,57] With respect to the system with apo-hTf, the relative amount of the binary species formed by 3-hydroxypyridine-2-carboxylate increases due to the lower strength of albumin than transferrin as a ligand toward the $V^{IV}O^{2+}$ ion.

The EPR spectrum of the system $V^{IV}O^{2+}$/Hprz/apo-hTf was recorded with a ratio 2:4:1, which ensures, in principle, the complete formation of $(VO)_2$(apo-hTf) or $[VO(prz)_2(H_2O)]$ depending on the relative donor strength of the protein and organic carrier toward $V^{IV}O^{2+}$. Trace b of Figure S15 of the Supporting Information shows that only $(VO)_2$(apo-hTf) (**I** in Figure S15) is formed at pH 7.40. No trace of $[VO(prz)_2(H_2O)]$ is detected (the two isomeric forms are indicated by **II** and **III** in trace c of Figure S15), suggesting that prz is much weaker than apo-hTf and is not able to compete with it for $V^{IV}O^{2+}$ binding. Analogous results were obtained with picCN and picFF, which behave similarly to prz. The low intensity of the EPR signal in the ternary system with apo-hTf indicates that at physiological pH part of $V^{IV}O^{2+}$ is present as a hydrolyzed species, EPR-silent; as observed with picFF, in these situations apo-hTf is not able to sequester all $V^{IV}O^{2+}$ and a significant amount remains bound to OH^- in polynuclear species. In contrast with picolinate, which forms with apo-hTf (VO)(apo-hTf)(pic) with the coordination of $VO(pic)^+$ to the specific iron-binding sites,[27c,d] pyrazine-2-carboxylate is too weak to compete with transferrin; thus, most of $V^{IV}O^{2+}$ is complexed as (VO)(apo-hTF)/$(VO)_2$(apo-hTf), whereas the remaining amount undergoes hydrolysis to form polynuclear $V^{IV}O$ species.

The EPR spectrum measured in the ternary system $V^{IV}O^{2+}$/Hprz/HSA 4:8:1 is represented in Figure S16 of the Supporting Information, trace b. It is different with respect to those recorded in the binary systems $V^{IV}O^{2+}$/HSA 4:1 and two shoulders are present, one at lower and another at higher fields than the resonances of $(VO)_x$(HSA) (**I** in Figure S16). The first species (**III** in Figure S16) is the mixed complex $VO(prz)_2$(HSA) (Scheme S3), as demonstrated by the coincidence of its absorptions and those of $[VO(prz)_2(1\text{-MeIm})]$ (**IV** in Figure S16). The *cis*-octahedral arrangement of

dx.doi.org/10.1021/ic500766t | *Inorg. Chem.* 2014, 53, 7960−7976

the bis-chelated species in solution, with an equatorial position occupied by a water molecule, favors the formation of the compounds in which His-N of an accessible residue replaces the weak H_2O ligand. This is also observed with picCN and in the systems containing HSA, holo-hTf, and IgG and insulin-mimetic compounds formed by maltol, ethylmaltol, kojic acid, picolinic acid, 1,2-dimethyl-3-hydroxy-4(1*H*)-pyridinone, and 2-hydroxypyridine-*N*-oxide.[25,27c,h,i] The absolute value of ^{51}V A_z calculated for $[VO(prz)_2(1\text{-MeIm})]$ is −2.5% lower than the experimental value, confirming the attribution proposed (Table 5). It is not possible to demonstrate if the isomer *OC*-6-24 or *OC*-6-23 or a mixture of them is formed. The species **II** may be a 1:1 species of prz with an equatorial binding of a His-N to give $VO(prz)(HSA)(H_2O)$ (Scheme S3, b). However, the possibility that **II** is the isomer *OC*-6-42 of $[VO(prz)_2(H_2O)]$ cannot be ruled out completely due to the coincidence of the M_I = 7/2 resonances of the two species (cf. traces b and d of Figure S16). In this case too, DFT simulations allowed us to assign the M_I = 7/2 resonances in the range 411−412 mT to $VO(prz)(HSA)(H_2O)$ rather than the deprotonated derivative $VO(prz)(HSA)(OH)$ (Table 5). Whereas the strong picolinate carrier forms with HSA mainly $VO(pic)_2(HSA)$ (*OC*-6-24 isomer with the equatorial coordination of a His-N), the weaker pyrazine-2-carboxylate ligand undergoes displacement reactions by HSA and solvent and, for this reason, $(VO)_x(HSA)$ and $VO(prz)(HSA)(H_2O)$, besides $VO(prz)_2(HSA)$, are formed at the experimental conditions used in this study.

CONCLUSIONS

Oxidovanadium(IV) complexes of 5-cyanopyridine-2-carboxylic acid (HpicCN) (**1**, **2**), 3,5-difluoropyridine-2-carboxylic acid (HpicFF) (**3**), 3-hydroxypyridine-2-carboxylic acid (H_2hypic) (**4**), and pyrazine-2-carboxylic acid (Hprz) (**5**) were synthesized in the presence of mild bases, such as calcium or sodium acetate salts. The study of the solid-state structures with X-ray diffraction analysis revealed the formation of *cis*-octahedral bis-chelated complexes with an (equatorial−equatorial) and (equatorial−axial) arrangement of the (N, COO^-) donor set of ligands and a water molecule (in **1**−**3**, **5**) or a carboxylic group of the Hhypic(−) ligand (**4**) coordinated in the fourth equatorial site in *cis* position to the V=O group. For this type of structure, four isomers are possible, indicated as *OC*-6-23, *OC*-6-24, *OC*-6-42, and *OC*-6-44 according to the IUPAC recommendations (Scheme 3). In the case of picCN, two different structures were determined depending on the crystallization conditions. Complex **1** presents the first crystallographic evidence for the formation of a *OC*-6-23 isomer for $V^{IV}O$ bis(picolinato) complexes with the two pyridine-N in *trans* position; **2**, **4**, and **5** possess the more common *OC*-6-24 arrangement, with two equatorial pyridine-N in *cis* position with respect to each other. In contrast with the known mononuclear and tetranuclear $V^{IV}O$ compounds of 3-hydroxypyridine-2-carboxylate (where it is coordinated to the vanadium metal center via the carboxylate and phenolate groups[18,52]), in compound **4** both Hhypic(−) ligands are coordinated with the (N, COO^-) couple, whereas the third ligand is coordinated monodentately via the carboxylate group. Interestingly, for **5** the structure of both enantiomers Δ and Λ was resolved.

DFT simulations suggest that in solution the stability of the two isomers *OC*-6-23 and *OC*-6-24 is comparable and that, among the isomers with two carboxylate-O in the equatorial plane, *OC*-6-42 is much more stable than *OC*-6-44; this supports the experimental evidence in an organic solvent or in aqueous solution, where only the EPR resonances of *OC*-6-42 are revealed together with those of isomers *OC*-6-24/*OC*-6-23. The attribution can be confirmed through the comparison between the experimental values of ^{51}V A_z and those calculated with Gaussian software.

$V^{IV}O$ compounds formed by picolinate derivatives appear to be very promising as potential insulin-enhancing agents.[12] With the perspective of testing these compounds in diabetes therapy as oral drugs, the thermodynamic stability and the biotransformation at physiological pH in the presence of the most important blood proteins, such as transferrin and albumin, were evaluated. The results depend on the strength of the ligands. In the systems containing apo-transferrin, with H_2hypic, the strongest ligand, $(VO)_2$(apo-hTf) coexists with $[VO(Hhypic)(hypic)]^-$, $[VO(hypic)_2]^{2-}$, and $[(VO)_4(\mu\text{-hypic})_4(H_2O)_4]$ whereas with the other three ligands $(VO)_2$(apo-hTf) is the main species in solution. In the systems with albumin, the mixed complexes $VOL_2(HSA)$ (isomer *OC*-6-24 or *OC*-6-23) and $VOL(HSA)(H_2O)$ are formed with picCN and prz, whereas $[VO(Hhypic)(hypic)]^-$, $[VO(hypic)_2]^{2-}$, and $[(VO)_4(\mu\text{-hypic})_4(H_2O)_4]$ with hypic and hydrolytic products with picFF predominate in aqueous solution.

An important observation concerns the low amount of $V^{IV}O$ species formed with hTf and HSA with the weakest ligand, picFF. This fact can be related to the formation of the polynuclear, hydrolytic complexes of the $V^{IV}O^{2+}$ ion (such as $[(VO)_2(OH)_5]^-$ and/or species with higher nuclearity), which hinder vanadium from binding to the specific sites of transferrin and to the unspecific sites of albumin. As a consequence, $V^{IV}O^{2+}$ cannot be sequestered by blood proteins (specifically hTf, which plays the most important role in the transport of pharmacologically active V compounds toward the target organs[23]) and exists in solution as hydroxido complexes; such species, due to their polynuclear structure, cannot cross the cell membranes, and a low insulin-mimetic action is expected.

The amount of $V^{IV}O^{2+}$ bound to the blood proteins can be related to the strength of the organic carrier used to complex vanadium. When the carrier L is weak, such as 3,5-difluoropyridine-2-carboxylate or 6-methylpicolinate,[27c] the hydrolysis predominates at physiological pH and the total V distributes between binary $V^{IV}O$−protein species ((VO)(apo-hTf)/$(VO)_2$(apo-hTF) with apo-hTf and $(VO)_x$HSA with HSA) and hydrolytic compounds ($[(VO)_2(OH)_5]^-$ and others with higher nuclearity). When the carrier L is intermediate, the capability of forming mixed $V^{IV}O$ species with the blood proteins depends on two factors: the structural features of the ligand and the geometry assumed at pH 7.40. When the carrier L is a synergistic anion, such as picolinate, (VO)(apo-hTf)(L) can be formed with the coordination of the cation VOL^+ to the specific iron-binding sites;[27c,d] when it is not a synergistic anion VOL_2(apo-hTf) and VOL_2(holo-hTf) are formed if the *cis*-octahedral species is stable at physiological pH (for example, with maltolate,[27f,i] ethylmaltolate,[27g] or kojate[27g]), or the $[VOL_2]$ compound remains intact in the case of square pyramidal geometry (for example, acetylacetonate[27c,i]). When carrier L is strong, such as 1,2-dimethyl-3-hydroxy-4(1*H*)-pyridinone,[27c,d,i] most of the $V^{IV}O^{2+}$ ions remain bound to the organic ligand. On this basis, it is expected that $V^{IV}O$ compounds formed by weak carriers do not enter the cells, whereas $V^{IV}O$ complexes formed by intermediate and strong carriers could cross the cellular membrane as VOL_2(holo-hTf),

dx.doi.org/10.1021/ic500766t | Inorg. Chem. 2014, 53, 7960−7976

which can be recognized by hTf receptors, and [VOL_2] via passive diffusion.[69]

All these considerations must be taken into account in the design of new V complexes with potential use in medicine.

■ ASSOCIATED CONTENT

Supporting Information

Tables S1−S13, Figures S1−S16, Schemes S1−S3, and CIF files giving crystallographic data for complexes **1**, **2**, **4**, and **5**. This material is available free of charge via the Internet at http://pubs.acs.org. CCDC 987887−987891 contain the supplementary crystallographic data for this paper. These data can be obtained free of charge via www.ccdc.cam.ac.uk/conts/retrieving.html (or from the Cambridge Crystallographic Data Centre, 12 Union Road, Cambridge CB21EZ, U.K.; fax: (+44) 1223-336-033 or e-mail: deposit@ccdc.cam.ac.uk).

■ AUTHOR INFORMATION

Corresponding Authors

*E-mail: franc.perdih@fkkt.uni-lj.si.

*E-mail: garribba@uniss.it.

Notes

The authors declare no competing financial interest.

■ ACKNOWLEDGMENTS

T.K.-D., A.M., and F.P. thank the Ministry of Education, Science and Sport of the Republic of Slovenia and the Slovenian Research Agency for financial support (P1-0230-0175) as well as the EN−FIST Centre of Excellence, Dunajska 156, 1000 Ljubljana, Slovenia, for the use of the Supernova diffractometer.

■ REFERENCES

(1) (a) Costa Pessoa, J.; Tomaz, I. *Curr. Med. Chem.* **2010**, *17*, 3701−3738. (b) Rehder, D. *Future Med. Chem.* **2012**, *4*, 1823−1837.

(2) (a) Thompson, K. H.; McNeill, J. H.; Orvig, C. *Chem. Rev.* **1999**, *99*, 2561−2572. (b) Thompson, K. H.; Orvig, C. *Coord. Chem. Rev.* **2001**, *219*−*221*, 1033−1053. (c) Shechter, Y.; Goldwaser, I.; Mironchik, M.; Fridkin, M.; Gefel, D. *Coord. Chem. Rev.* **2003**, *237*, 3−11. (d) Kawabe, K.; Yoshikawa, Y.; Adachi, Y.; Sakurai, H. *Life Sci.* **2006**, *78*, 2860−2866. (e) Sakurai, H.; Yoshikawa, Y.; Yasui, H. *Chem. Soc. Rev.* **2008**, *37*, 2383−2392.

(3) Nilsson, J.; Shteinman, A. A.; Degerman, E.; Enyedy, E. A.; Kiss, T.; Behrens, U.; Rehder, D.; Nordlander, E. *J. Inorg. Biochem.* **2011**, *105*, 1795−1800.

(4) Rehder, D. *Bioinorganic Vanadium Chemistry*; John Wiley & Sons Ltd.: Chichester, 2008.

(5) (a) Thompson, K. H.; Orvig, C. In *Metal Ions in Biological Systems*; Sigel, H.; Sigel, A., Eds.; Marcel Dekker: New York, 2004; Vol. *41*, pp 221−252. (b) Thompson, K. H.; Orvig, C. *J. Inorg. Biochem.* **2006**, *100*, 1925−1935.

(6) Thompson, K. H.; Lichter, J.; LeBel, C.; Scaife, M. C.; McNeill, J. H.; Orvig, C. *J. Inorg. Biochem.* **2009**, *103*, 554−558.

(7) Carroll, J., http://www.fiercebiotech.com/story/akesis-shutters-program-files-chap-7/2009-01-22.

(8) Wei, Y.; Zhang, C.; Zhao, P.; Yang, X.; Wang, K. *J. Inorg. Biochem.* **2011**, *105*, 1081−1085.

(9) Zhang, L.; Zhang, Y.; Xia, Q.; Zhao, X. M.; Cai, H. X.; Li, D. W.; Yang, X. D.; Wang, K.; Xia, Z. L. *Food Chem. Toxicol.* **2008**, *46*, 2996−3002.

(10) Nilsson, J.; Degerman, E.; Haukka, M.; Lisensky, G. C.; Garribba, E.; Yoshikawa, Y.; Sakurai, H.; Enyedy, E. A.; Kiss, T.; Esbak, H.; Rehder, D.; Nordlander, E. *Dalton Trans.* **2009**, 7902−7911.

(11) (a) Adachi, Y.; Yoshida, J.; Kodera, Y.; Katoh, A.; Takada, J.; Sakurai, H. *J. Med. Chem.* **2006**, *49*, 3251−3256. (b) Hiromura, M.; Adachi, Y.; Machida, M.; Hattori, M.; Sakurai, H. *Metallomics* **2009**, *1*, 92−100.

(12) (a) Sakurai, H.; Fujii, K.; Fujimoto, S.; Fujisawa, Y.; Takechi, K.; Yasui, H. In *Vanadium Compounds: Chemistry, Biochemistry and Therapeutic Applications*; American Chemical Society: Washington, DC, 1998; Vol. *711*, pp 344−352. (b) Sakurai, H. In *Vanadium: The Versatile Metal*; American Chemical Society: Washington, DC, 2007; Vol. *974*, pp 110−120.

(13) Sakurai, H.; Fujii, K.; Watanabe, H.; Tamura, H. *Biochem. Biophys. Res. Commun.* **1995**, *214*, 1095−1101.

(14) (a) Fujimoto, S.; Fujii, K.; Yasui, H.; Matsushita, R.; Takada, J.; Sakurai, H. *J. Clin. Biochem. Nutr.* **1997**, *23*, 113−129. (b) Fujisawa, Y.; Sakurai, H. *Chem. Pharm. Bull.* **1999**, *47*, 1668−1670.

(15) Sakurai, H.; Tamura, A.; Takino, T.; Ozutsumi, K.; Kawabe, K.; Kojima, Y. *Inorg. React. Mech.* **2000**, *2*, 69−77.

(16) Takino, T.; Yasui, H.; Yoshitake, A.; Hamajima, Y.; Matsushita, R.; Takada, J.; Sakurai, H. *J. Biol. Inorg. Chem.* **2001**, *6*, 133−142.

(17) Sasagawa, T.; Yoshikawa, Y.; Kawabe, K.; Sakurai, H.; Kojima, Y. *J. Inorg. Biochem.* **2002**, *88*, 108−112.

(18) (a) Yano, S.; Nakai, M.; Sekiguchi, F.; Obata, M.; Kato, M.; Shiro, M.; Kinoshita, I.; Mikuriya, M.; Sakurai, H.; Orvig, C. *Chem. Lett.* **2002**, *31*, 916−917. (b) Nakai, M.; Obata, M.; Sekiguchi, F.; Kato, M.; Shiro, M.; Ichimura, A.; Kinoshita, I.; Mikuriya, M.; Inohara, T.; Kawabe, K.; Sakurai, H.; Orvig, C.; Yano, S. *J. Inorg. Biochem.* **2004**, *98*, 105−112.

(19) Gätjens, J.; Meier, B.; Kiss, T.; Nagy, E. M.; Buglyó, P.; Sakurai, H.; Kawabe, K.; Rehder, D. *Chem.−Eur. J.* **2003**, *9*, 4924−4935.

(20) Gätjens, J.; Meier, B.; Adachi, Y.; Sakurai, H.; Rehder, D. *Eur. J. Inorg. Chem.* **2006**, 3575−3585.

(21) Esbak, H.; Enyedy, E. A.; Kiss, T.; Yoshikawa, Y.; Sakurai, H.; Garribba, E.; Rehder, D. *J. Inorg. Biochem.* **2009**, *103*, 590−600.

(22) Willsky, G. R.; Chi, L.-H.; Godzala, M., III; Kostyniak, P. J.; Smee, J. J.; Trujillo, A. M.; Alfano, J. A.; Ding, W.; Hu, Z.; Crans, D. C. *Coord. Chem. Rev.* **2011**, *255*, 2258−2269.

(23) (a) Kiss, T.; Jakusch, T.; Hollender, D.; Dörnyei, A. In *Vanadium: The Versatile Metal*; Kustin, K.; Costa Pessoa, J.; Crans, D. C., Eds.; American Chemical Society: Washington, DC, 2007; Vol. *974*, pp 323−339. (b) Kiss, T.; Jakusch, T.; Hollender, D.; Dornyei, A.; Enyedy, E. A.; Costa Pessoa, J.; Sakurai, H.; Sanz-Medel, A. *Coord. Chem. Rev.* **2008**, *252*, 1153−1162. (c) Jakusch, T.; Costa Pessoa, J.; Kiss, T. *Coord. Chem. Rev.* **2011**, *255*, 2218−2226.

(24) Willsky, G. R.; Goldfine, A. B.; Kostyniak, P. J.; McNeill, J. H.; Yang, L. Q.; Khan, H. R.; Crans, D. C. *J. Inorg. Biochem.* **2001**, *85*, 33−42.

(25) Liboiron, B. D.; Thompson, K. H.; Hanson, G. R.; Lam, E.; Aebischer, N.; Orvig, C. *J. Am. Chem. Soc.* **2005**, *127*, 5104−5115.

(26) (a) Jakusch, T.; Hollender, D.; Enyedy, E. A.; Gonzalez, C. S.; Montes-Bayon, M.; Sanz-Medel, A.; Costa Pessoa, J.; Tomaz, I.; Kiss, T. *Dalton Trans.* **2009**, 2428−2437. (b) Correia, I.; Jakusch, T.; Cobbinna, E.; Mehtab, S.; Tomaz, I.; Nagy, N. V.; Rockenbauer, A.; Costa Pessoa, J.; Kiss, T. *Dalton Trans.* **2012**, *41*, 6477−6487. (c) Mehtab, S.; Gonçalves, G.; Roy, S.; Tomaz, A. I.; Santos-Silva, T.; Santos, M. F. A.; Romão, M. J.; Jakusch, T.; Kiss, T.; Costa Pessoa, J. *J. Inorg. Biochem.* **2013**, *121*, 187−195. (d) Gonçalves, G.; Tomaz, A. I.; Correia, I.; Veiros, L. F.; Castro, M. M. C. A.; Avecilla, F.; Palacio, L.; Maestro, M.; Kiss, T.; Jakusch, T.; Garcia, M. H. V.; Costa Pessoa, J. *Dalton Trans.* **2013**, *42*, 11841−11861. (e) Costa Pessoa, J.; Gonçalves, G.; Roy, S.; Correia, I.; Mehtab, S.; Santos, M. F. A.; Santos-Silva, T. *Inorg. Chim. Acta* **2014**, *420*, 60−68.

(27) (a) Sanna, D.; Garribba, E.; Micera, G. *J. Inorg. Biochem.* **2009**, *103*, 648−655. (b) Sanna, D.; Micera, G.; Garribba, E. *Inorg. Chem.* **2009**, *48*, 5747−5757. (c) Sanna, D.; Micera, G.; Garribba, E. *Inorg. Chem.* **2010**, *49*, 174−187. (d) Sanna, D.; Buglyó, P.; Micera, G.; Garribba, E. *J. Biol. Inorg. Chem.* **2010**, *15*, 825−839. (e) Sanna, D.; Micera, G.; Garribba, E. *Inorg. Chem.* **2011**, *50*, 3717−3728. (f) Sanna, D.; Biro, L.; Buglyo, P.; Micera, G.; Garribba, E. *Metallomics* **2012**, *4*, 33−36. (g) Sanna, D.; Bíró, L.; Buglyó, P.; Micera, G.; Garribba, E. *J. Inorg. Biochem.* **2012**, *115*, 87−99. (h) Sanna, D.; Ugone, V.; Micera,

G.; Garribba, E. *Dalton Trans.* **2012**, *41*, 7304−7318. (i) Sanna, D.; Micera, G.; Garribba, E. *Inorg. Chem.* **2013**, *52*, 11975−11985.
(28) Santos, M. F. A.; Correia, I.; Oliveira, A. R.; Garribba, E.; Pessoa, J. C.; Santos-Silva, T. *Eur. J. Inorg. Chem.* **2014**, DOI: 10.1002/ejic.201402408.
(29) Yoshikawa, Y.; Sakurai, H.; Crans, D. C.; Micera, G.; Garribba, E. *Dalton Trans.* **2014**, *43*, 6965−6972.
(30) Chasteen, N. D.; Grady, J. K.; Holloway, C. E. *Inorg. Chem.* **1986**, *25*, 2754−2760.
(31) Putnam, F. W. In *The Plasma Proteins*, 2nd ed.; Putnam, F. W., Ed.; Academic Press: New York, 1984; pp 45−166.
(32) Gran, G. *Acta Chem. Scand.* **1950**, *4*, 559−577.
(33) Irving, H. M.; Miles, M. G.; Pettit, L. D. *Anal. Chim. Acta* **1967**, *38*, 475−488.
(34) Gans, P.; Sabatini, A.; Vacca, A. *J. Chem. Soc., Dalton Trans.* **1985**, 1195−1200.
(35) Henry, R. P.; Mitchell, P. C. H.; Prue, J. E. *J. Chem. Soc., Dalton Trans.* **1973**, 1156−1159.
(36) Davies, C. W. *J. Chem. Soc.* **1938**, 2093−2098.
(37) (a) Komura, A.; Hayashi, M.; Imanaga, H. *Bull. Chem. Soc. Jpn.* **1977**, *50*, 2927−2931. (b) Vilas Boas, L. F.; Costa Pessoa, J. In *Comprehensive Coordination Chemistry*; Wilkinson, G.; Gillard, R. D.; McCleverty, J. A., Eds.; Pergamon Press: Oxford, 1985; Vol. 3, pp 453−583.
(38) *CrysAlis PRO*; Agilent Technologies: Yarnton, 2011.
(39) Sheldrick, G. M. *Acta Crystallogr., Sect. A* **2008**, *64*, 112−122.
(40) Altomare, A.; Burla, M. C.; Camalli, M.; Cascarano, G. L.; Giacovazzo, C.; Guagliardi, A.; Moliterni, A. G. G.; Polidori, G.; Spagna, R. *J. Appl. Crystallogr.* **1999**, *32*, 115−119.
(41) Frisch, M. J.; Trucks, G. W.; Schlegel, H. B.; Scuseria, G. E.; Robb, M. A.; Cheeseman, J. R.; Montgomery, J. A., Jr.; Vreven, T.; Kudin, K. N.; Burant, J. C.; Millam, J. M.; Iyengar, S. S.; Tomasi, J.; Barone, V.; Mennucci, B.; Cossi, M.; Scalmani, G.; Rega, N.; Petersson, G. A.; Nakatsuji, H.; Hada, M.; Ehara, M.; Toyota, K.; Fukuda, R.; Hasegawa, J.; Ishida, M.; Nakajima, T.; Honda, Y.; Kitao, O.; Nakai, H.; Klene, M.; Li, X.; Knox, J. E.; Hratchian, H. P.; Cross, J. B.; Adamo, C.; Jaramillo, J.; Gomperts, R.; Stratmann, R. E.; Yazyev, O.; Austin, A. J.; Cammi, R.; Pomelli, C.; Ochterski, J. W.; Ayala, P. Y.; Morokuma, K.; Voth, G. A.; Salvador, P.; Dannenberg, J. J.; Zakrzewski, V. G.; Dapprich, S.; Daniels, A. D.; Strain, M. C.; Farkas, O.; Malick, D. K.; Rabuck, A. D.; Raghavachari, K.; Foresman, J. B.; Ortiz, J. V.; Cui, Q.; Baboul, A. G.; Clifford, S.; Cioslowski, J.; Stefanov, B. B.; Liu, G.; Liashenko, A.; Piskorz, P.; Komaromi, I.; Martin, R. L.; Fox, D. J.; Keith, T.; Al-Laham, M. A.; Peng, C. Y.; Nanayakkara, A.; Challacombe, M.; Gill, P. M. W.; Johnson, B.; Chen, W.; Wong, M. W.; Gonzalez, C.; Pople, J. A. *Gaussian 03*, revision C.02; Gaussian, Inc.: Wallingford, CT, 2004.
(42) (a) Bühl, M.; Kabrede, H. *J. Chem. Theory Comput.* **2006**, *2*, 1282−1290. (b) Bühl, M.; Reimann, C.; Pantazis, D. A.; Bredow, T.; Neese, F. *J. Chem. Theory Comput.* **2008**, *4*, 1449−1459.
(43) Micera, G.; Garribba, E. *Int. J. Quantum Chem.* **2012**, *112*, 2486−2498.
(44) (a) Micera, G.; Pecoraro, V. L.; Garribba, E. *Inorg. Chem.* **2009**, *48*, 5790−5796. (b) Micera, G.; Garribba, E. *Eur. J. Inorg. Chem.* **2010**, 4697−4710. (c) Gorelsky, S.; Micera, G.; Garribba, E. *Chem.−Eur. J.* **2010**, *16*, 8167−8180. (d) Lodyga-Chruscinska, E.; Micera, G.; Garribba, E. *Inorg. Chem.* **2011**, *50*, 883−899. (e) Micera, G.; Garribba, E. *J. Comput. Chem.* **2011**, *32*, 2822−2835. (f) Sanna, D.; Varnágy, K.; Timári, S.; Micera, G.; Garribba, E. *Inorg. Chem.* **2011**, *50*, 10328−10341. (g) Micera, G.; Garribba, E. *Eur. J. Inorg. Chem.* **2011**, 3768−3780. (h) Sanna, D.; Buglyó, P.; Bíró, L.; Micera, G.; Garribba, E. *Eur. J. Inorg. Chem.* **2012**, 1079−1092. (i) Sanna, D.; Pecoraro, V.; Micera, G.; Garribba, E. *J. Biol. Inorg. Chem.* **2012**, *17*, 773−790. (j) Pisano, L.; Varnagy, K.; Timári, S.; Hegetschweiler, K.; Micera, G.; Garribba, E. *Inorg. Chem.* **2013**, *52*, 5260−5272. (k) Sanna, D.; Várnagy, K.; Lihi, N.; Micera, G.; Garribba, E. *Inorg. Chem.* **2013**, *52*, 8202−8213. (l) Lodyga-Chruscinska, E.; Szebesczyk, A.; Sanna, D.; Hegetschweiler, K.; Micera, G.; Garribba, E. *Dalton Trans.* **2013**, *42*, 13404−13416. (m) Justino, G.; Garribba, E.; Costa Pessoa, J. *J. Biol. Inorg. Chem.* **2013**, *18*, 803−813.
(45) (a) Miertuš, S.; Scrocco, E.; Tomasi, J. *Chem. Phys.* **1981**, *55*, 117−129. (b) Miertuš, S.; Tomasi, J. *Chem. Phys.* **1982**, *65*, 239−245. (c) Cossi, M.; Barone, V.; Cammi, R.; Tomasi, J. *Chem. Phys. Lett.* **1996**, *255*, 327−335.
(46) Lodyga-Chruscinska, E.; Sanna, D.; Garribba, E.; Micera, G. *Dalton Trans.* **2008**, 4903−4916.
(47) *Nomenclature of Inorganic Chemistry−IUPAC Recommendations*; Connelly, N. G.; Damhus, T.; Hartshorn, R. M.; Hutton, A. T., Eds.; The Royal Society of Chemistry: Cambridge, 2005.
(48) Allen, F. H.; Kennard, O. *Chem. Des. Autom. News* **1993**, *8*, 31−37.
(49) Melchior, M.; Thompson, K. H.; Jong, J. M.; Rettig, S. J.; Shuter, E.; Yuen, V. G.; Zhou, Y.; McNeill, J. H.; Orvig, C. *Inorg. Chem.* **1999**, *38*, 2288−2293.
(50) McLauchlan, C. C.; Hooker, J. D.; Jones, M. A.; Dymon, Z.; Backhus, E. A.; Greiner, B. A.; Dorner, N. A.; Youkhana, M. A.; Manus, L. M. *J. Inorg. Biochem.* **2010**, *104*, 274−281.
(51) Okabe, N.; Muranishi, Y. *Acta Crystallogr. Sect. E* **2002**, *58*, m287−m289.
(52) Kiss, E.; Bényei, A.; Kiss, T. *Polyhedron* **2003**, *22*, 27−33.
(53) Cevik, S.; Şaşmaz, B.; Poyraz, M.; Sarı, M.; Büyükgüngör, O. *J. Chem. Crystallogr.* **2011**, *41*, 796−800.
(54) Ooi, S.; Nishizawa, M.; Matsumoto, K.; Kuroya, H.; Saito, K. *Bull. Chem. Soc. Jpn.* **1979**, *52*, 452−457.
(55) Nakamoto, K. *Infrared and Raman Spectra of Inorganic and Coordination Compounds*, 3rd ed.; John Wiley & Sons: New York, 1978.
(56) (a) Julien-Cailhol, N.; Rose, E.; Vaisserman, J.; Rehder, D. *J. Chem. Soc., Dalton Trans.* **1996**, 2111−2115. (b) Yang, L.; la Cour, A.; Anderson, O. P.; Crans, D. C. *Inorg. Chem.* **2002**, *41*, 6322−6331. (c) Smee, J. J.; Epps, J. A.; Teissedre, G.; Maes, M.; Harding, N.; Yang, L.; Baruah, B.; Miller, S. M.; Anderson, O. P.; Willsky, G. R.; Crans, D. C. *Inorg. Chem.* **2007**, *46*, 9827−9840. (d) Hazra, A.; Gupta, S.; Roy, S.; Mandal, T. N.; Das, K.; Konar, S.; Jana, A.; Ray, S.; Butcher, R. J.; Kar, S. K. *Polyhedron* **2011**, *30*, 187−194. (e) Wong, H. W.; Lo, K. M.; Ng, S. W. *Acta Crystallogr. Sect. E* **2011**, *67*, m799−m799.
(57) Kiss, E.; Petrohán, K.; Sanna, D.; Garribba, E.; Micera, G.; Kiss, T. *Polyhedron* **2000**, *19*, 55−61.
(58) Kiss, E.; Garribba, E.; Micera, G.; Kiss, T.; Sakurai, H. *J. Inorg. Biochem.* **2000**, *78*, 97−108.
(59) Kiss, T.; Kiss, E.; Garribba, E.; Sakurai, H. *J. Inorg. Biochem.* **2000**, *80*, 65−73.
(60) (a) Chasteen, D. N. In *Biological Magnetic Resonance*; Berliner, L. J. J.; Reuben, J., Eds.; Plenum Press: New York, 1981; Vol. 3, pp 53−119. (b) Smith, T. S., II; LoBrutto, R.; Pecoraro, V. L. *Coord. Chem. Rev.* **2002**, *228*, 1−18.
(61) Micera, G.; Garribba, E. *Dalton Trans.* **2009**, 1914−1918.
(62) Garribba, E.; Micera, G.; Lodyga-Chruscinska, E.; Sanna, D. *Eur. J. Inorg. Chem.* **2006**, 2690−2700.
(63) Sanna, D.; Buglyo, P.; Tomaz, A. I.; Pessoa, J. C.; Borovic, S.; Micera, G.; Garribba, E. *Dalton Trans.* **2012**, *41*, 12824−12838.
(64) Buglyó, P.; Kiss, E.; Fábián, I.; Kiss, T.; Sanna, D.; Garribba, E.; Micera, G. *Inorg. Chim. Acta* **2000**, *306*, 174−183.
(65) (a) Buglyo, P.; Kiss, T.; Kiss, E.; Sanna, D.; Garribba, E.; Micera, G. *J. Chem. Soc., Dalton Trans.* **2002**, 2275−2282. (b) Rangel, M.; Leite, A.; João Amorim, M.; Garribba, E.; Micera, G.; Lodyga-Chruscinska, E. *Inorg. Chem.* **2006**, *45*, 8086−8097.
(66) Neese, F. *Coord. Chem. Rev.* **2009**, *253*, 526−563.
(67) Sun, H.; Cox, M.; Li, H.; Sadler, P. *Struct. Bonding (Berlin)* **1997**, *88*, 71−102.
(68) Garribba, E.; Micera, G.; Lodyga-Chruscinska, E.; Sanna, D.; Sanna, G. *Eur. J. Inorg. Chem.* **2005**, 4953−4963.
(69) (a) Sanna, D.; Serra, M.; Micera, G.; Garribba, E. *Inorg. Chem.* **2014**, *53*, 1449−1464. (b) Sanna, D.; Serra, M.; Micera, G.; Garribba, E. *Inorg. Chim. Acta* **2014**, *420*, 75−84.
(70) (a) Thompson, K. H.; Battell, M.; McNeill, J. H. In *Vanadium in the Environment, Part 2: Health Effects*; Nriagu, J. O., Ed.; Wiley, New

York, 1998; pp 21−37. (b) Rehder, D.; Costa Pessoa, J.; Geraldes, C.; Castro, M.; Kabanos, T.; Kiss, T.; Meier, B.; Micera, G.; Pettersson, L.; Rangel, M.; Salifoglou, A.; Turel, I.; Wang, D. *J. Biol. Inorg. Chem.* **2002**, *7*, 384−396. (c) Sakurai, H.; Fugono, J.; Yasui, H. *Mini-Rev. Med. Chem.* **2004**, *4*, 41−48.